

## INFORMATION TO USERS

This manuscript has been reproduced from the microfilm master. UMI films the text directly from the original or copy submitted. Thus, some thesis and dissertation copies are in typewriter face, while others may be from any type of computer printer.

**The quality of this reproduction is dependent upon the quality of the copy submitted.** Broken or indistinct print, colored or poor quality illustrations and photographs, print bleedthrough, substandard margins, and improper alignment can adversely affect reproduction.

In the unlikely event that the author did not send UMI a complete manuscript and there are missing pages, these will be noted. Also, if unauthorized copyright material had to be removed, a note will indicate the deletion.

Oversize materials (e.g., maps, drawings, charts) are reproduced by sectioning the original, beginning at the upper left-hand corner and continuing from left to right in equal sections with small overlaps. Each original is also photographed in one exposure and is included in reduced form at the back of the book.

Photographs included in the original manuscript have been reproduced xerographically in this copy. Higher quality 6" x 9" black and white photographic prints are available for any photographs or illustrations appearing in this copy for an additional charge. Contact UMI directly to order.



Bell & Howell Information and Learning  
300 North Zeeb Road, Ann Arbor, MI 48106-1346 USA  
800-521-0600



**UNIVERSITY OF ALBERTA**

**THE LAST GLACIATION AND RELATIVE SEA LEVEL  
HISTORY OF CENTRAL BAUMANN FIORD,  
SOUTHWEST ELLESMERE ISLAND,  
CANADIAN HIGH ARCTIC**

By

**NIGEL ATKINSON**



A thesis submitted to the Faculty of Graduate Studies and Research in partial  
fulfillment of the requirements for the degree of Master of Science

Department of Earth and Atmospheric Science

Edmonton, Alberta

Spring 1999



National Library  
of Canada

Acquisitions and  
Bibliographic Services

395 Wellington Street  
Ottawa ON K1A 0N4  
Canada

Bibliothèque nationale  
du Canada

Acquisitions et  
services bibliographiques

395, rue Wellington  
Ottawa ON K1A 0N4  
Canada

*Your file Votre référence*

*Our file Notre référence*

The author has granted a non-exclusive licence allowing the National Library of Canada to reproduce, loan, distribute or sell copies of this thesis in microform, paper or electronic formats.

The author retains ownership of the copyright in this thesis. Neither the thesis nor substantial extracts from it may be printed or otherwise reproduced without the author's permission.

L'auteur a accordé une licence non exclusive permettant à la Bibliothèque nationale du Canada de reproduire, prêter, distribuer ou vendre des copies de cette thèse sous la forme de microfiche/film, de reproduction sur papier ou sur format électronique.

L'auteur conserve la propriété du droit d'auteur qui protège cette thèse. Ni la thèse ni des extraits substantiels de celle-ci ne doivent être imprimés ou autrement reproduits sans son autorisation.

0-612-40025-5

# UNIVERSITY OF ALBERTA

## LIBRARY RELEASE FORM

**Name of Author:** Nigel Atkinson  
**Title of Thesis:** The last glaciation and relative sea level  
history of central Baumann Fiord,  
southwest Ellesmere Island, Canadian  
high Arctic  
**Degree:** Master of Science  
**Year this Degree Granted:** 1999

Permission is hereby granted to the University of Alberta Library to reproduce single copies of this thesis and to lend or sell such copies for private, scholarly or scientific research purposes only.

The author reserves all other publication and other rights in association with the copyright in the thesis, and except as hereinbefore provided, neither the thesis nor any substantial portion thereof may be printed or otherwise reproduced in any material form whatever without the author's prior written permission.

*Nigel Atkinson*

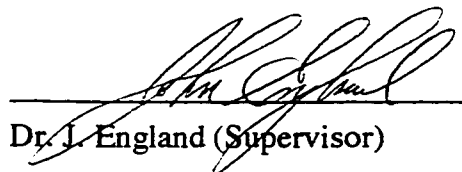
Nigel Atkinson  
31 Whiston Lane  
Huyton  
Liverpool  
L36 1TX  
United Kingdom

14<sup>TH</sup> DECEMBER 1998

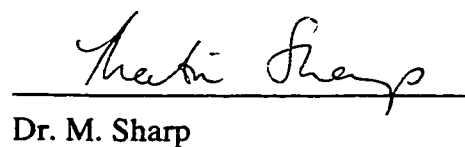
# University of Alberta

## Faculty of Graduate Studies And Research

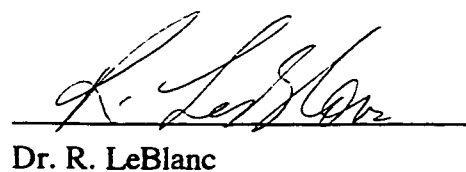
The undersigned certify that they have read, and recommend to the Faculty of Graduate Studies and Research for acceptance, a thesis entitled "The Last Glaciation and Relative Sea Level History of central Baumann Fiord, southwest Ellesmere Island, Canadian High Arctic" submitted by Nigel Atkinson in partial fulfillment of the requirements for the degree of Master of Science.



Dr. J. England (Supervisor)



Dr. M. Sharp



Dr. R. LeBlanc

Date: JANUARY 15<sup>TH</sup> 1999

**This thesis is dedicated with love and thanks to Mum and Dad.**

## **ABSTRACT**

Baumann Fiord is a major re-entrant on southwest Ellesmere Island, measuring >100 km long, and 20 km wide. This thesis reconstructs the glacial and sea level history of central Baumann Fiord, based on surficial geological mapping, interpretations of glacial landforms and associated sediments, surveys on raised marine deposits and radiocarbon dating marine shells. Striated bedrock, and the distribution of granite erratics throughout the study area record the inundation of central Baumann Fiord with ice from the Prince of Wales Icefield, and its SW advance across Bjorne Peninsula, en route to Norwegian Bay.

Deglacial marine sediments (dating  $\leq 9.3$  ka BP) distributed along Baumann Fiord record the entry of marine fauna, occasioned by the progressive retreat of trunk ice during the early Holocene. Collectively, these data suggest extensive ice cover on southwest Ellesmere Island during the Last Glacial Maximum.

Geomorphic and sedimentary signatures indicate that the removal of trunk ice from Baumann Fiord facilitated retreat of tributary glaciers occupying Svendsen and Bjorne peninsulas. Deglaciation was likely promoted by both ongoing eustatic sea level rise and well documented early Holocene warming. Geomorphic evidence records the progressive retreat of terrestrial ice margins from the coast of Baumann Fiord to the interior of southwest Ellesmere Island, from  $\sim 8.5$  ka BP.

Isobases drawn on the 8.0 ka shoreline for central Baumann Fiord exhibit a rise to the NW, towards Eureka Sound. The isobase pattern indicates that during the Late Wisconsinan, the thickest ice in the region occupied Eureka Sound.



## ACKNOWLEDGEMENTS

For the opportunity to work in the high Arctic, I am indebted to my supervisor, Dr. John England. From the summer of 1997 on Ellesmere Island, to the completion of this thesis, my two years in Canada have been a personal and academic experience that I shall always remember. For your hospitality, enthusiasm, rigorous editing and good humour, John, I offer you my thanks.

Valuable comments on this thesis were made by my committee members, Drs. Raymond LeBlanc and Martin Sharp. Particular thanks are due to Dr. Martin Sharp for his patience and willingness to discuss various aspects of this thesis over the last year. Financial support for this thesis was provided by the Canadian Circumpolar Institute (BAR Grants) and the Natural Sciences and Engineering Research Council of Canada (Grant #A6608 to J. England). My research on southwest Ellesmere Island would have been impossible without the excellent logistical support provided by the Polar Continental Shelf Project. Murray Unick provided able and enthusiastic field assistance, and good company during our life in the Logan. I would also like to thank Dr. Colm Ó Cofaigh, who provided much appreciated help at the beginning of my first field season, and sacrificed two hats in the search of elusive striae.

Throughout my academic life, I am fortunate to have been taught by a number of dedicated individuals. Don Jacobson and Chris Moore, St. Margarets High School, Liverpool provided the early stimulus to pursue a career in Earth sciences, through their enthusiasm for fieldwork, and infectious interest in the subject. Dr. David Evans, University of Glasgow stimulated further interest, and the completion of this thesis is in large part due to his continued encouragement. I am also grateful to Drs. Rod Smith and Scott Lamoureux, who have always had time to answer my endless stream of questions over the last two years, and provided valuable advice on the logistics involved in Arctic fieldwork.

I have so many happy memories from the last two years at U of A, in the company of good friends and other graduate students in the department. In particular Luke, Trudy, Anthony, Wendy, Klaus, Ingrid, Jens and Stephanie. Special thanks to Rod Smith and Sandra Mackay-Smith for their continued friendship and hospitality, and Dr. Robert and B.J. Busch who have done much to make my life in Edmonton so comfortable.

To Lana Bzdel, a great big thank you. With your continual love, support, hugs, cups of coffee and humour, you helped me remember that there was a life beyond this thesis.

Finally, to the two people who have played the largest role in helping me complete this thesis, my parents (Alf and Diane Atkinson) for their love and spiritual support throughout my life. With their honesty, wisdom and humour, they have been with me every step of the way, always encouraging me to pursue my dreams. Thank you.

# TABLE OF CONTENTS

Chapter	Page
1. INTRODUCTION AND RATIONALE	1
1.1 Introduction	1
1.2 Previous Research	1
1.3 Project Rationale	8
1.4 Research Objectives	8
1.5 Physiography and field sites	10
1.6 Geology	14
1.7 Climate	14
2. METHODOLOGY AND TECHNIQUES	17
2.1 Introduction	17
2.2 Research Methods	
2.2.1 <i>Surficial Mapping</i>	17
2.2.2 <i>Establishing the age and elevation of former sea levels</i>	19
3. THE QUATERNARY GLACIAL HISTORY OF CENTRAL BAUMANN FIORD	22
3.1 Introduction	22
3.2 Rock and Residuum	22
3.2.1 <i>Associated Landforms</i>	24
3.3 Till	24
3.3.1 <i>Provenance of erratics</i>	33
3.3.2 <i>Associated Landforms</i>	33
3.4 Glaciofluvial Sediments and Landforms	36
3.5 Raised Marine Sediments	37
3.5.1 <i>Deltaic, beach and nearshore sediments</i>	37

3.6 Alluvium	38
3.7 Colluvium	40
3.8 Summary	40
 4. THE LATE QUATERNARY DEGLACIAL HISTORY OF CENTRAL BAUMANN FIORD	 42
4.1 Introduction	42
4.2 Deglaciation in Svarte Fiord	42
4.3 Deglaciation in central Baumann Fiord	46
4.3.1 <i>Eastern Svendsen Peninsula and Hoved Island</i>	46
4.3.2 <i>Southern Bjorne Peninsula</i>	50
4.4 Terrestrial Deglaciation	52
4.4.1 <i>Eastern Svendsen Peninsula</i>	52
4.4.2 <i>Southern Bjorne Peninsula</i>	52
4.5 Discussion	59
4.6 Summary	65
 5. CONCLUSIONS	 66
5.1 Last Glacial Maximum	66
5.2 Relative Sea Level History	69
5.3 Future Research	69
 6. REFERENCES	 72

## LIST OF TABLES

Table	Page
4.1 Holocene radiocarbon dates, central Baumann Fiord	45

# LIST OF FIGURES

<b>Figures</b>	<b>Page</b>
1.1 Regional map of the Queen Elizabeth Islands	2
1.2 Central and western Ellesmere Island and eastern Axel Heiberg Island	4
1.3 Geology map of the Queen Elizabeth Islands	7
1.4 Satellite image showing the physiography of SW Ellesmere Island	11
1.5 SW Ellesmere Island showing location of Baumann Fiord and adjacent field areas	12
1.6 Bathymetric chart of Baumann Fiord	13
3.1 Distribution of surficial sediments and glacial landforms on E. Svendsen Peninsula, Hoved Island and S. Bjorne Peninsula	23
3.2 Unweathered dolomitic limestone overlain by till veneer on E. Svendsen Peninsula	25
3.3 Striae on Hoved Island	26
3.4 Granite erratic on surface of till veneer, E. Svendsen Peninsula	28
3.5 Granite erratic in limestone blockfield, highlands of E. Svendsen Peninsula	29
3.6 Granite erratic, head of Eids Fiord	30
3.7 Granite erratic in till blanket, highlands of S. Bjorne Peninsula	31
3.8 Limestone erratics, lowlands of south-central Bjorne Peninsula	32
3.9 Thin section of granite from Hoved Island, showing possible source area	34
3.10 Thin section of granite from S. Bjorne Peninsula, showing possible source area	35
3.11 Rectangular polygons in nearshore marine sediment, S. Bjorne Peninsula	39
4.1a Marine limit elevation, central Baumann Fiord	43
4.1b Distribution of deglacial landforms, central Baumann Fiord	44
4.2 Airphoto showing <i>M-1</i>	47
4.3 Oblique photograph of <i>M-1</i>	48
4.4 Washing limit, E. Svendsen Peninsula	49
4.5 Photograph of section <i>S-1</i>	51
4.6 Fine-grained nearshore sediments distal to delta <i>D-4</i>	53

4.7a Photograph of <i>S-2</i>	54
4.7b Photograph of <i>S-2</i> (continued)	55
4.8 Coarse silt exhibiting cross-lamination in <i>S-2</i>	56
4.9 Gravel interbed in unit of coarse silt, section <i>S-2</i>	57
4.10 Dropstone contacts in <i>S-2</i>	58
4.11 Kame moraine <i>M-2</i>	60
4.12 Airphoto of delta <i>D-5</i>	61
 5.1 Regional map of eastern Ellesmere Island	 68
5.2 Isobase map drawn on the 8.0 ka shoreline in central Baumann Fiord	70

# CHAPTER ONE

## 1.1 Introduction

This chapter summarizes models previously invoked to explain the style of glaciation within the Queen Elizabeth Islands (QEI; Figure 1.1) during the last glacial maximum (LGM). For two decades, researchers debated whether the glacial geologic evidence, combined with the magnitude and pattern of postglacial emergence, recorded an Innuitian Ice Sheet inundating the QEI, or whether it recorded the Franklin Ice Complex, which involved less extensive glacier advances, 5-60 km beyond the margins of contemporary ice caps (Blake, 1970, 1972; England, 1976a and b; England, 1987; Tushingham, 1991; England *et al.*, 1991). Recent fieldwork in the central and high Canadian Arctic resolves this debate by demonstrating the existence of the Innuitian Ice Sheet (Ó Cofaigh, 1997, 1998a and b; England, 1998a, in press; Bednarski, 1998; Dyke, in press a and b).

Fieldwork presented in this thesis concerns the glacial and sea level history of SW Ellesmere Island, and both tests and refines this regional revision by investigating the style and chronology of glaciation in central Baumann Fiord (Figure 1.2).

## 1.2 Previous Research

Blake (1970, 1972) proposed that during the LGM, the QEI were covered by the Innuitian Ice Sheet, which coalesced with the Laurentide Ice Sheet to the south, and the Greenland Ice Sheet to the east. This reconstruction was based primarily on the pattern of Holocene emergence and the distribution of radiocarbon-dated marine molluscs throughout the QEI (England, 1976a, in press). Blake (1970, 1975) identified large quantities of dacitic pumice deposited 5.1 ka BP along a raised beach on the north shore of Jones Sound (Figure 1.1). This strandline is now delevelled, and tilts upwards to the NW. Elsewhere, the 5 ka BP strandline reaches a maximum elevation along a broad NE-SW axis extending from Bathurst Island to Eureka Sound (Figure 1.1). These data were collectively interpreted to record the axis of maximum glacioisostatic unloading, where the Innuitian Ice Sheet was formerly thickest. Blake (1970, 1972) also recognized a decrease in the age of radiocarbon-dated marine molluscs from the western QEI (~12 ka



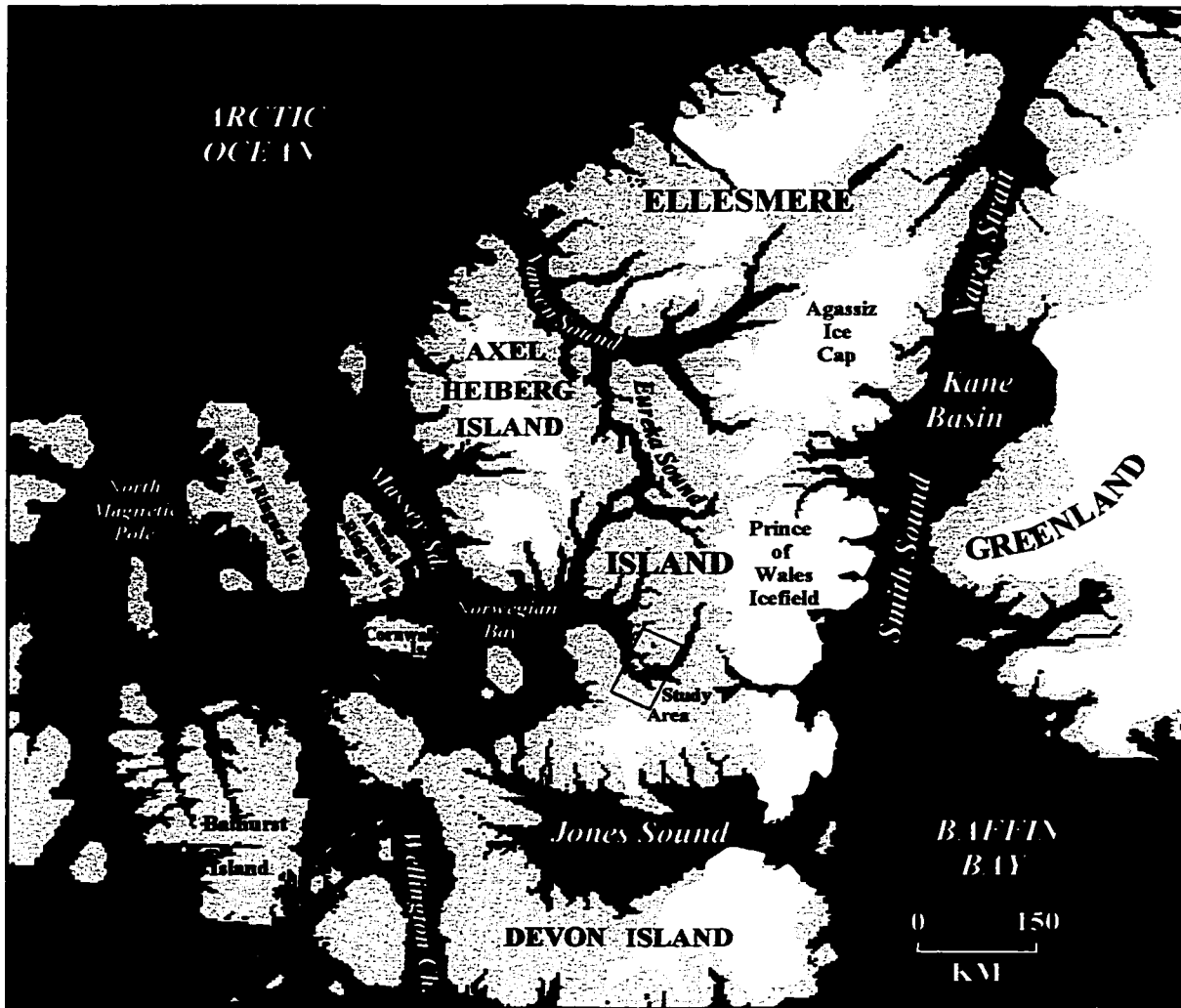


Figure 1.1. Regional map showing the Queen Elizabeth Islands, Arctic Canada, and the adjacent coast of Greenland. Contemporary ice caps are shaded.

BP) towards Eureka Sound (9-8 ka BP). Blake proposed that the entry of the marine fauna was facilitated by the retreat of the Innuitian Ice Sheet, which progressively evacuated the channels of the QEI. Furthermore, on SE Ellesmere Island, Blake (1977, 1992) and Blake *et al.* (1996) suggested that glacial sculpture along Smith Sound and on Carey Øer, N Baffin Bay (Figures 1.1 and 5.1) provided evidence that Smith Sound was filled by a 1500 m thick ice stream, formed by coalescent Ellesmere and Greenland ice during the LGM (the Smith Sound Ice Stream).

Other investigations of glacial and early Holocene raised marine sediments and landforms on Ellesmere Island were interpreted to indicate that the QEI were not occupied by the Innuitian Ice Sheet, but rather by discontinuous ice caps. These were collectively referred to as the Franklin Ice Complex (England, 1976a; Dyke and Prest, 1987; Sloan, 1990; Bell, 1992, 1996). Within the peripheral depression, beyond the margins of the Franklin Ice Complex, England (1983, 1992) proposed that the fiords were occupied by a full glacial Innuitian Sea, which remained stable, close to marine limit, prior to the onset of ice retreat at ~8 ka BP.

Hodgson (1985) identified a 500 km long "drift belt" composed of ice-marginal landforms contacting Holocene glaciomarine sediments at the heads of many fiords in west-central Ellesmere Island (Figure 1.2). These were deposited 5 to 60 km west of contemporary glacier margins by the coalesced predecessor of the Agassiz, Prince of Wales and Sydkap ice caps (Figure 1.2). Radiocarbon-dated shells recovered from glaciomarine sediments along the drift belt indicated that glacier retreat occurred  $\geq 8.8$  ka BP. The interpretation that the position and chronology of the drift belt recorded the last ice limit on west-central Ellesmere Island supported the Franklin Ice Complex (Model B, Hodgson, 1985; England, 1990; Sloan, 1990; Bell, 1996). However, Hodgson (1985) also noted that distal to the drift belt, striated and moulded bedrock was overlain by till and Holocene glaciomarine sediment. Hodgson suggested that the limit of the last glaciation lay at least 20 km beyond the heads of Bay, Strathcona and Vandom fiords (Figure 1.2) but found no unequivocal evidence of pervasive ice in west-central Ellesmere Island or Eureka Sound during the LGM.

Hodgson (1985) suggested that the eastward retreat of ice margins from the head of Starfish Bay (Figure 1.2) indicated that the Braskeruds Plain was a significant ice source in west-central Ellesmere Island during the LGM. Hodgson (1985) reasoned that if the palaeoglaciation level at the LGM was below the elevation of the Braskeruds Plain, then much larger areas of Ellesmere, Devon and Axel Heiberg islands would have been glaciated than suggested by the Franklin Ice Complex. Furthermore, Hodgson (1985)

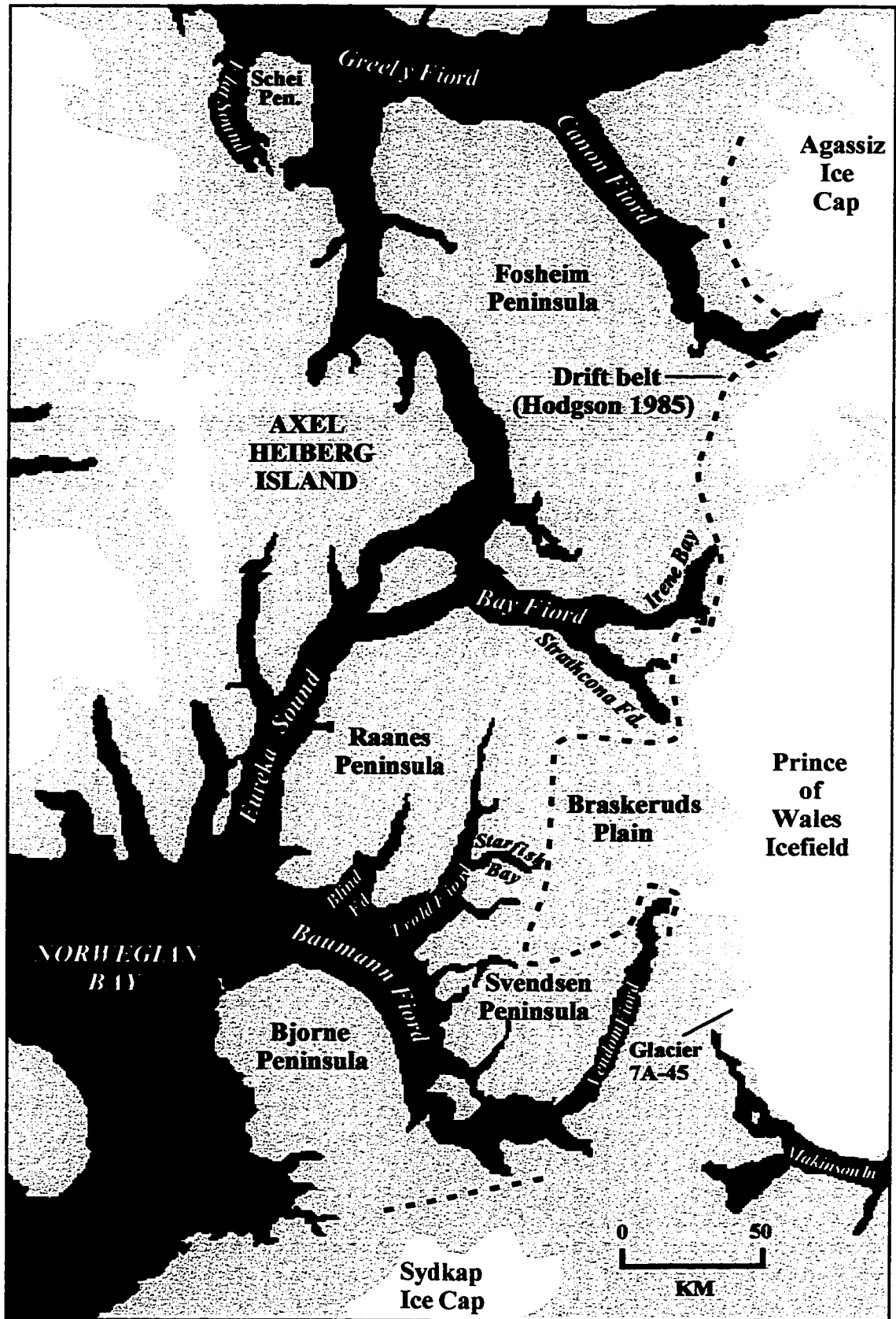


Figure 1.2. Central and western Ellesmere Island and eastern Axel Heiberg Island showing contemporary ice caps (shaded) and position of the drift belt

remarked that no radiocarbon evidence of a transgressive shoreline associated with a full glacial sea (the Innuitian Sea; England, 1992) had been found in the outer fiords of west-central Ellesmere Island or Eureka Sound. Hodgson concluded that neither a pan-archipelago ice sheet or discontinuous ice caps adequately explained the style of glaciation in the region during the LGM.

Erratics of Greenland provenance examined along a 500 km transect of E Ellesmere Island document the former contact between Greenland and Ellesmere ice along Nares Strait (England, 1998a; Figure 1.1). Deglaciation of Nares Strait and E Ellesmere Island is recorded by lateral meltwater channels along the former margin of the trunk glacier that filled Nares Strait, and by moraines in the tributary valleys of E Ellesmere Island, into which local ice retreated. The distribution of Holocene shells throughout Nares Strait also records the sequential re-entry of the sea, from both the north and south, which is consistent with the geomorphic evidence for ice retreat (England, 1998a). Collectively, these data support the inundation of Nares Strait by glaciers during the LGM (cf., Blake, 1992; Funder and Hansen, 1996).

Bednarski (1998) reported that during the LGM, NE Axel Heiberg Island was covered by glaciers emanating from both local and regional sources. Lateral meltwater channels grading to Holocene ice-contact deltas record ice retreat from the coast of Axel Heiberg Island to contemporary ice sources in the western highlands (Figure 1.1). This evidence suggests that NE Axel Heiberg Island was glaciated by local ice during the LGM. However, glacial flutings on Schei Peninsula, the low isthmus that separates the head of Flat Sound from Eureka Sound, are orientated NNW, signifying that ice from Eureka Sound flowed at least as far as Flat Sound (Figure 1.2). These data are also associated with NNW trending striae and till exhibiting a N-S fabric on central and NE Schei Peninsula, respectively (Figure 1.2). Bednarski (1998) concluded that this area was dominated by regional ice-flow from Eureka Sound, which was thick enough to override Schei Peninsula. Ice-marginal landforms and ice-flow features suggest that local and regional glaciers coalesced, at least during early Holocene deglaciation. Furthermore, Bednarski (1998) observed that Holocene marine limit rises from NE Axel Heiberg Island towards Eureka Sound. This indicates that the centre of maximum glacioisostatic unloading in the region occurs towards northern Eureka Sound.

Ó Cofaigh (1997) recognized that Raanes Peninsula, west-central Ellesmere Island (Figure 1.2) was also inundated by glaciers originating from regional and local sources. Field mapping demonstrated that the distribution of granite erratics across Raanes Peninsula related to a regional dispersal train extending through Bay Fiord (Bell,

1992) and southern Eureka Sound, and an undefined train through Baumann Fiord (Figure 1.2). These erratics can be traced back to the crystalline terrain underlying the Prince of Wales Icefield (Figure 1.3). Ó Cofaigh (1997) remarked that the scarcity of granite erratics on southern Raanes Peninsula indicated a southward deflection of the Baumann Fiord dispersal train, likely a result of local ice-flow from Raanes Peninsula. Surface exposure dates on granite erratics from these dispersal trains and adjacent bedrock cluster between 11 and 21 ka BP (Ó Cofaigh, 1998b). Moreover, the association of granite erratics with marine limit sediments indicates that ice responsible for granite dispersal retreated during the early Holocene (Ó Cofaigh, 1998b). Ó Cofaigh (1997) proposed that the high Holocene marine limit on Raanes Peninsula related to glacioisostatic recovery from a loading centre in southern Eureka Sound. This interpretation is supported by isobases drawn on the 8.5 ka BP shoreline for the eastern QEI, which show a centre of maximum glacioisostatic unloading encircling Eureka Sound (England and Ó Cofaigh, 1998).

Dyke (in press a) suggests that the glacial geologic record of Devon Island (Figure 1.1) also supports regional glaciation during the LGM. Dyke proposes that weakly fluted till and striae trending NW-SE on Baillie-Hamilton and Beachy islands were produced by a SE flowing ice stream centred through Wellington Channel (Figure 1.1). Moreover, weak to moderate glacial scouring and fluted till on W. Devon Island indicate that local ice emanating from a divide over the axis of the island was deflected SW, as it approached Wellington Channel. Dyke (in press b) proposes that the Wellington Channel Ice Stream was sustained by southward flowing Innuitian ice from a NE-SW trending divide extending across the central QEI, and diverted westward ice-flow from Devon Island. Deglaciation of the Wellington Channel Ice Stream occurred during the early Holocene (Dyke, in press a). Furthermore, lateral meltwater channels, interpreted to have been eroded during the last glaciation, record the retreat of local ice towards the former divide on Devon Island (Dyke, in press a).

Collectively, these interpretations provide a new consensus concerning the glacial history of the QEI during the LGM (England, 1998b). Confirmation of the presence of thick ice in Nares Strait, as well as Nansen and Eureka sounds, and its southward extension into the central Arctic Islands and Wellington Channel, supports the Innuitian Ice Sheet hypothesis (cf., Blake, 1970, 1972, 1992).

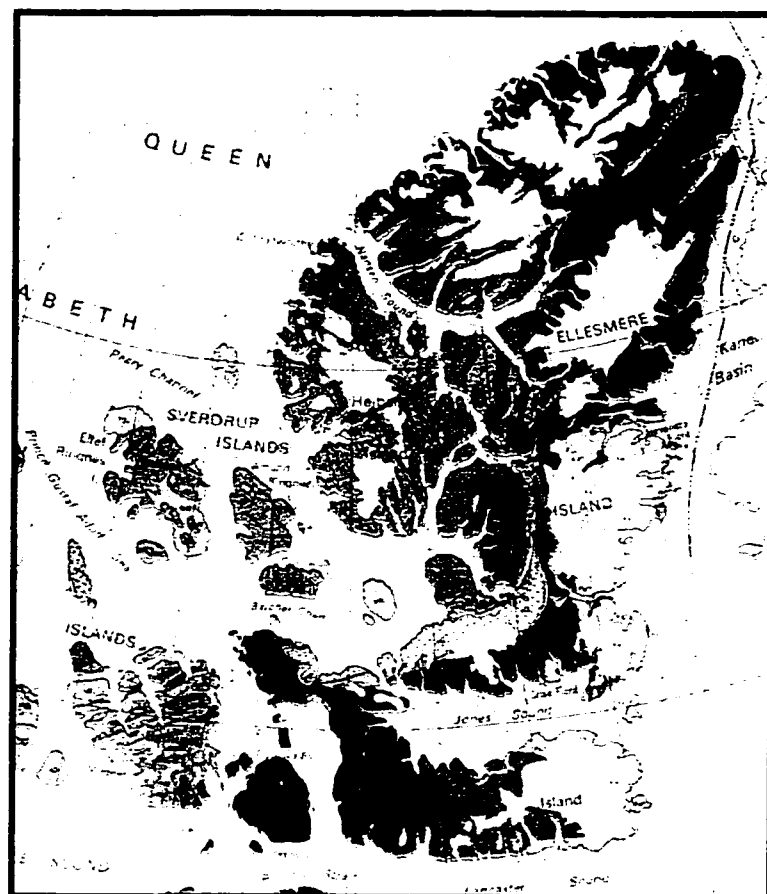



Figure 1.3. Geology map of the Queen Elizabeth Islands  
(Geological Survey of Canada, 1970)

#### TERTIARY

 Shale, clay, sandstone,  
limestone


#### CRETACEOUS

 Sandstone, shale


#### JURASSIC

 Sandstone

#### TRIASSIC

 Calcareous  
siltstone,  
shale

#### PERMIAN

 Sandstone, limestone,  
conglomerate

#### DEVONIAN

 Sandy  
limestone

#### ORDOVICIAN

 Limestone


#### PALAEOZOIC

 Dolomitic  
siltstone

#### ORDOVICIAN/SILURIAN

 Dolomitic  
limestone

#### ARCHAEAN

 Crystalline  
rocks, mainly granite and gneiss

## 1.3 Project Rationale

A significant implication of the reconstruction presented by England (1998a) is that the style and extent of glaciation in W Ellesmere Island was influenced by the filling of Nares Strait by glacier ice during the LGM. England (1998a) proposed that Greenland ice in Nares Strait buttressed E Ellesmere Island ice, diminishing its surface gradient and hence outflow along its eastern flank. England (1998a) suggested that this would have promoted thickening of the Ellesmere Island ice divide, regionally involving the Prince of Wales Icefield, causing a strengthening of westward ice-flow towards Eureka Sound (Figure 1.1). Geological evidence for strengthened westerly ice-flow is now recognized in the mapping of granite dispersal through Bay and Baumann fiords, which is attributed to the LGM (Ó Cofaigh, 1997, 1998b; England, 1998a; England and Ó Cofaigh, 1998; Figure 1.2).

To date, there have been only reconnaissance field studies concerning the glacial and sea level history of SW Ellesmere Island (cf., Hodgson, 1985). This represents a substantial gap in the regional database. Fieldwork in central Baumann Fiord provides an opportunity to address the regional revision further, and examine the evidence for enhanced westward flow from E Ellesmere Island.

## 1.4 Research Objectives

The objectives of this thesis are threefold, and are designed to refine our understanding of the glacial and sea level history of central Baumann Fiord, SW Ellesmere Island (Figure 1.2).

### *1) To determine the extent and origin of former glaciation in central Baumann Fiord*

Investigating the style and chronology of glaciation in central Baumann Fiord is an important objective of this research. Prior to this study, the style and provenance of glaciation on SW Ellesmere Island was uncertain. Possible ice sources included the NE margin of the Laurentide Ice Sheet (Hättestrand and Stroeve, 1996), westward flowing Ellesmere ice from the Prince of Wales Icefield and Sydkap Ice Cap, or local plateau glaciers. Central Baumann Fiord lies close to the inferred zone of maximum thickness of the Innuitian Ice Sheet (Blake, 1970). Furthermore, the location, orientation and

bathymetry of Baumann Fiord make it a likely outlet for the westward advance of glaciers from the Ellesmere Island ice divide, regionally involving the Prince of Wales Icefield (Ó Cofaigh, 1997, 1998b; England, 1998a; Figure 1.2). Central Baumann Fiord is also in close proximity to the Sydkap Ice Cap and a postulated ice source over Braskeruds Plain (cf., Hodgson, 1985; Figure 1.2). Therefore, Baumann Fiord is centrally located to assess the relative contribution of regional and local ice sources on the glacial history of SW Ellesmere Island. By integrating the extent, configuration and origin of ice-flow through central Baumann Fiord, it will be possible to delineate former ice divides and outlets of the Innuitian Ice Sheet in SW Ellesmere Island.

*2) To determine the dynamics of ice retreat in central Baumann Fiord*

Clarifying the history of ice retreat in central Baumann Fiord provides further insight into the response of High Arctic glaciers to palaeoenvironmental change. Ó Cofaigh (1998a) and England (1998a, in press) propose a two-step model of ice retreat around W and E Ellesmere Island, respectively. The paucity of geomorphic evidence indicative of extensive glaciation is attributed to the rapid break-up of marine-based ice, either initiated or enhanced by calving, in response to rapid eustatic sea level rise. Subsequent stabilization on adjacent coastlines may account for prominent glaciogenic landforms at the heads of many fiords in west-central Ellesmere Island (e.g., the drift belt; Hodgson, 1985). Research in central Baumann Fiord, focusing particularly on the chronology of initial marine transgression, would help to determine whether a similar pattern of retreat occurred in SW Ellesmere Island, as occurred to the N and E (Ó Cofaigh, 1998a; England, 1998a).

*3) To determine the magnitude, pattern and age of sea level adjustments associated with former ice load changes*

The magnitude and pattern of postglacial emergence is routinely used as a proxy to estimate former ice thickness (cf., Tushingham, 1991) and its application in central Baumann Fiord is relevant to the determination of the regional glacial loading history of SW Ellesmere Island (cf., Andrews, 1970). Furthermore, determining the magnitude and chronology of sea level adjustments in central Baumann Fiord will extend the emergence database further southward, from Eureka Sound, and provide data necessary to refine regional isobase maps, which define centres of maximum glacioisostatic



unloading (cf., England, 1976a and b, 1990; Hodgson, 1985; Bell, 1992; Ó Cofaigh, 1997, 1998c). The rate and pattern of Holocene sea level change can also be used to test whether other factors contributed to regional emergence, such as neotectonics (cf. England, 1997). Moreover, radiocarbon age determinations on raised marine sediments are intimately related to the deglacial history of central Baumann Fiord (Objective 2).

## 1.5 Physiography and Field Sites

The physiography of SW Ellesmere Island marks a transition between the low relief ( $\leq 300$  metres above sea level; m asl) of the central QEI, and the mountains that surround Eureka Sound ( $> 1400$  m asl) and underlie the Prince of Wales Icefield ( $> 1700$  m asl; Figures 1.1 and 1.4). Baumann Fiord is a major embayment orientated NW-SE on SW Ellesmere Island (Figure 1.2). It is  $> 100$  km long and reaches a width of 20 km at its mouth, where it converges with Eureka Sound and Norwegian Bay (Figure 1.5). The bathymetry of Baumann Fiord is complex because Hoved Island divides the channel into two basins (Canadian Hydrographic Service, 1985; Figure 1.6). Outer Baumann Fiord, west of Hoved Island, is characterized by a  $> 350$  m deep, elongate channel that deepens towards Norwegian Bay. Inner Baumann Fiord, east of Hoved Island, is an enclosed, elliptically-shaped basin, 200-250 m deep. A shoal that rises to within 7 m of contemporary sea level occurs adjacent to W. Hoved Island (Figure 1.6).

Fieldwork was conducted from June to August (1997) at three field sites along a N-S transect across central Baumann Fiord (Figure 1.5). The northernmost site on E Svendsen Peninsula ( $77^{\circ} 40' \text{ N}$ ,  $84^{\circ} 15' \text{ W}$ ) borders the north shore of Baumann Fiord, and occupies a 25 km wide and 30 km long lowland ( $\leq 200$  m asl). The lowland is surrounded to the east and west by ridges  $> 600$  m in relief. These comprise the NE-SW trending anticlines, which enclose Vendom and Svarte fiords (Figure 1.4). Svarte Fiord extends for 30 km, with parallel coasts  $\sim 2.5$  km apart (Figure 1.6). The east coast consists of spectacular limestone cliffs ( $> 600$  m), which are part of the anticlinal highlands, whereas the west coast is characterized by low-relief ( $\leq 300$  m). The Prince of Wales Icefield lies  $\sim 50$  km to the east, and the Braskeruds Plain  $\sim 70$  km to the north of Svendsen Peninsula (Figure 1.2). The second field site, Hoved Island ( $77^{\circ} 32' \text{ N}$ ,  $85^{\circ} 14' \text{ W}$ ) is  $15 \text{ km}^2$  and consists of two NE-SW trending anticlines that have a relief of  $\sim 300$  m (Figure 1.6). These ridges terminate as steep coastal cliffs at the north and south ends of the island, and enclose a 13 km wide lowland ( $\leq 200$  m asl). The southern field site on Bjorne Peninsula ( $77^{\circ} 15' \text{ N}$ ,  $85^{\circ} 30' \text{ W}$ ) borders the south shore of

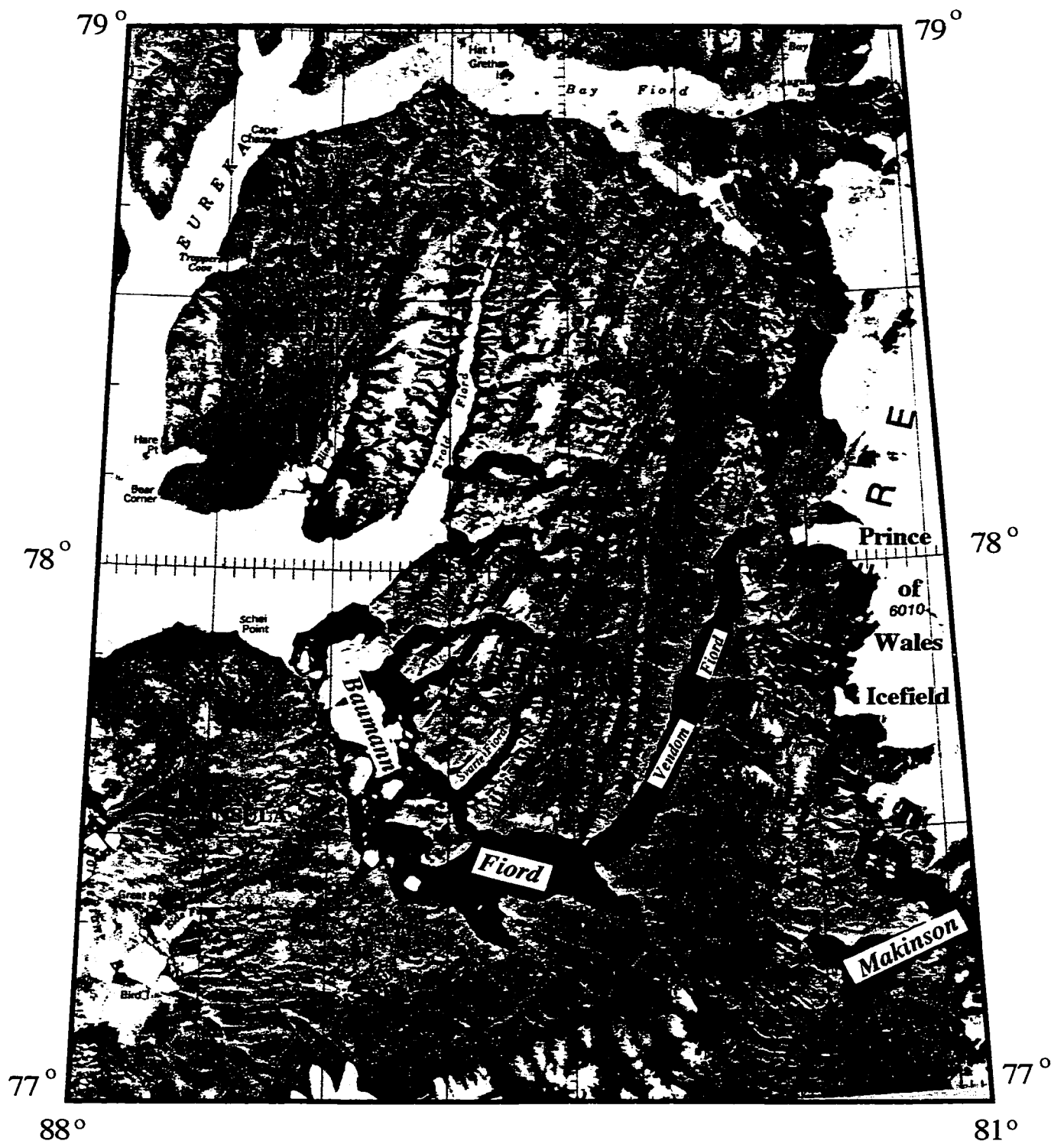


Figure 1.4. Satellite image showing the physiography of southwest Ellesmere Island  
(Canadian Topographic Survey, 1975)

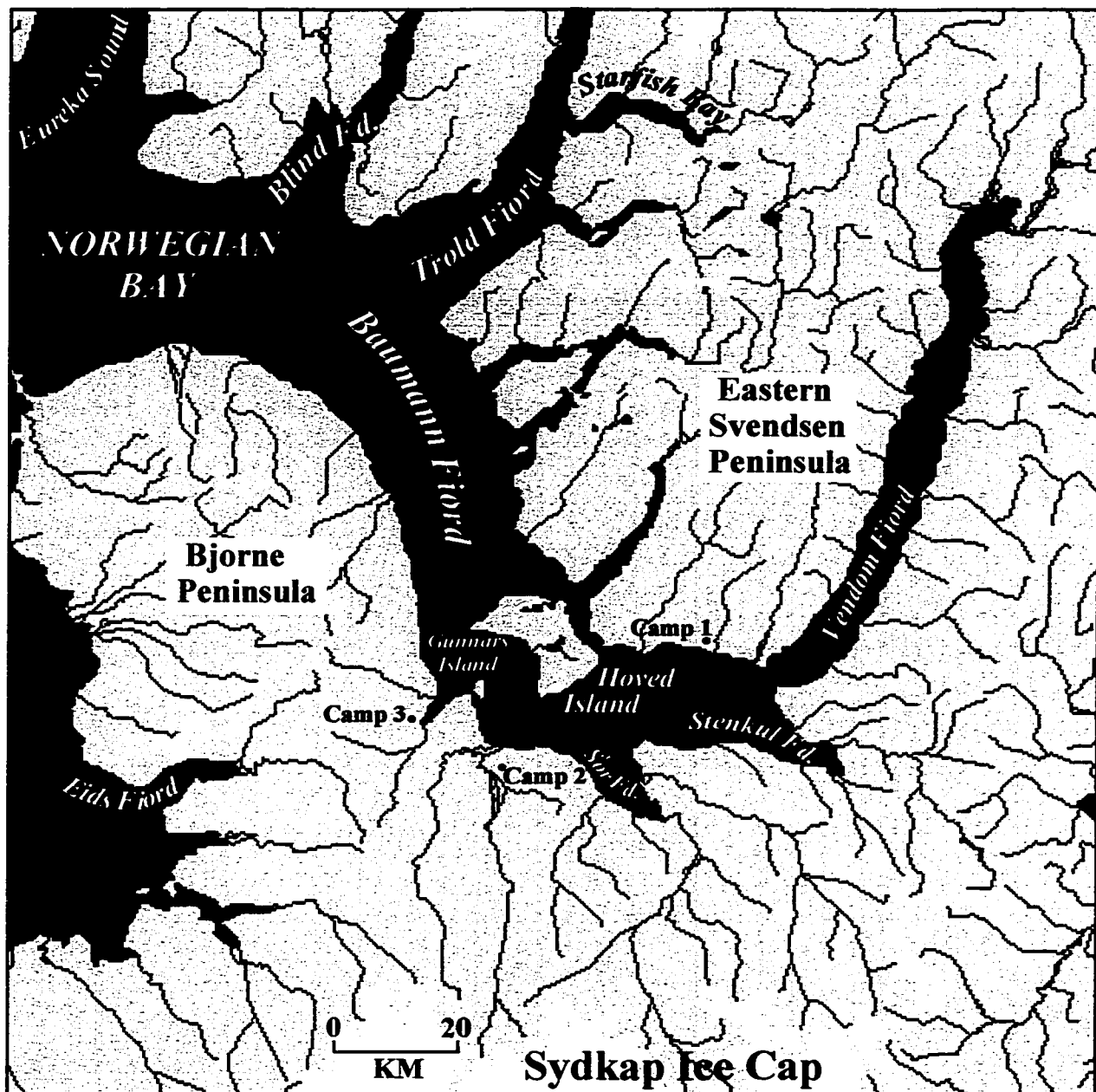


Figure 1.5. Southwest Ellesmere Island showing location of Baumann Fiord and adjacent field areas

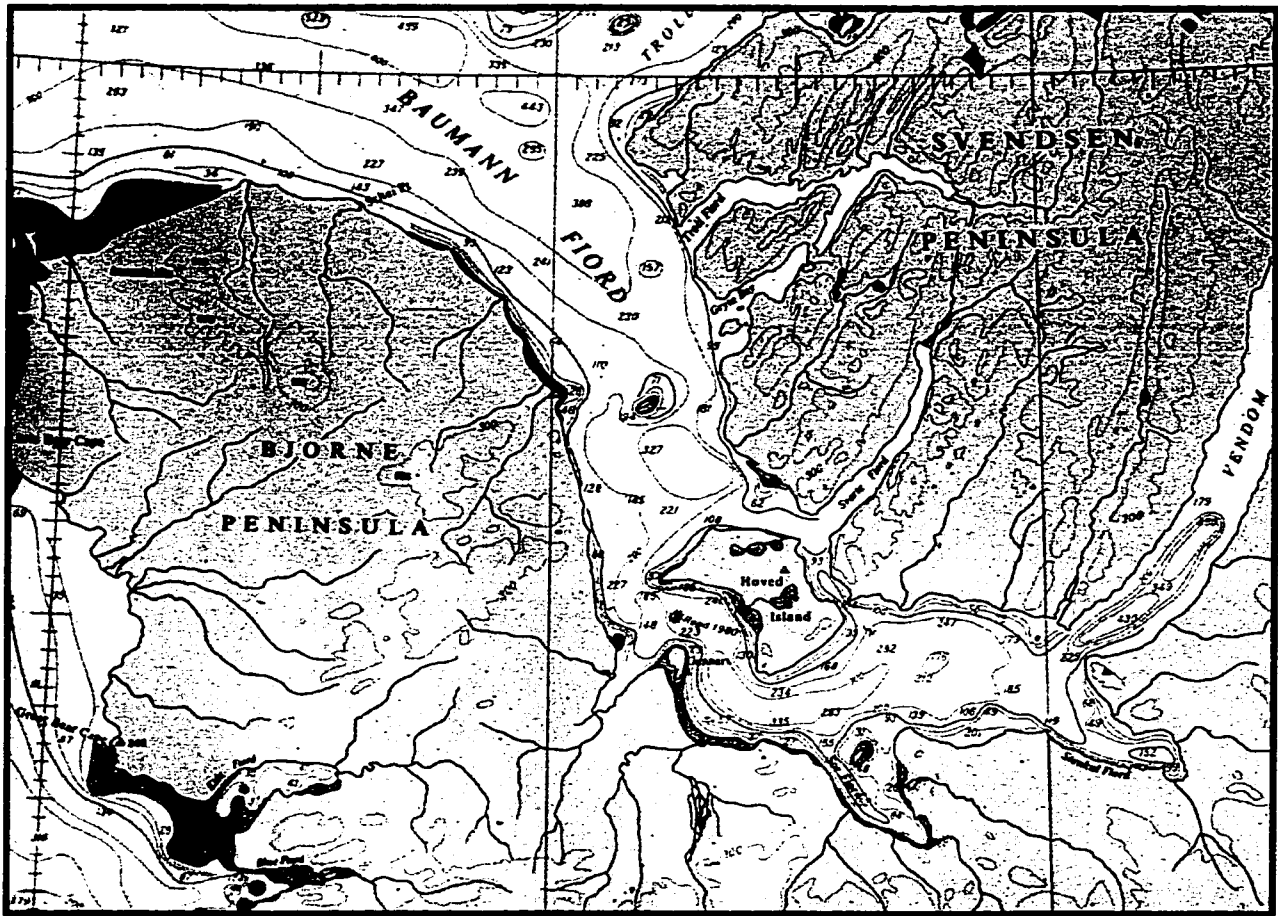


Figure 1.6. The bathymetry of Baumann Fiord (Canadian Hydrographic Service, 1985)

Baumann Fiord (Figure 1.5). This area consists of a ~50 km<sup>2</sup> lowland (<150 m asl) which abuts the E-W trending Schei Syncline (Figure 1.4). These highlands (>700 m asl) support the Sydkap Ice Cap, 35 km to the south (Figure 1.5). The eastern limit of the field area consists of uplands (>300 m asl) that flank the west coast of Sor Fiord. Collectively, the three field areas have a diverse topography, ranging from coastal lowlands to steep inter-fiord highlands.

## 1.6 Geology

The physiography of E Svendsen Peninsula, Hoved Island and S Bjorne Peninsula is dictated by its structural geology, which imparts the NE-SW grain (Figure 1.4). The entire field area occurs within the Franklinian Mobile Belt, an Upper to Middle Palaeozoic carbonate and clastic sedimentary succession, deformed during the Ellesmerian Orogeny (Trettin, 1987; Figure 1.3). Kerr (1981) remarked that Tertiary tectonic rifting augmented this structural trend. The Canadian Shield outcrops ~80 km to the east, in the Prince of Wales Mountains, where granitic rocks form nunataks (Figure 1.3; Frisch, 1988).

The lowlands of E Svendsen Peninsula display outcrops of dolomitic limestone which belong to the Allen Bay Formation (Upper Ordovician to Middle Silurian; Mayr, 1973; Figure 1.3). The sandy limestones of the Bird Fiord Formation (Middle Devonian) overlie the Allen Bay Formation (Figure 1.3). Hoved Island displays similar lithological and structural elements to E Svendsen Peninsula (Figure 1.3).

Southern Bjorne Peninsula displays more diverse lithologies (Figure 1.3). The Allen Bay Formation borders the south shore of central Baumann Fiord. Overlying these to the SW are calcareous shale and siltstones of the Eids Formation (Lower to Middle Devonian). In the southern part of the field area, bioclastic and variably dolomitic limestones belonging to the Blue Fiord Formation (Middle Devonian) form linear tors, paralleling the Schei Syncline (Figure 1.4). Consequently, at all field sites, crystalline erratics transported from the Canadian Shield are conspicuous.

## 1.7 Climate

Baumann Fiord separates the northern and northwestern climatic regions (Maxwell, 1981). A northern subregion encompasses Nansen and Eureka sounds and

their adjacent lowlands (Figure 1.1). This subregion is highly continental, with few outside climatic influences, because the mountains of Ellesmere and Axel Heiberg islands prevent the incursion of storm tracks originating from Baffin Bay and the Arctic Ocean (Maxwell, 1981; Figure 1.1). The rain shadow effect in this subregion results in the lowest mean annual precipitation in Canada (64 mm at Eureka) and high summer insolation (greatest mean annual temperature range in the Arctic Islands: 43° C at Eureka, Alt and Maxwell, 1990).

Southwest Ellesmere Island is in close proximity to the northwestern climatic region, which encompasses Norwegian Bay (Figures 1.1 and 1.2; Maxwell, 1981). Because the rainshadow to the north does not extend to SW Ellesmere Island, central Baumann Fiord is characterized by a maritime arctic climate which is similar to that of the Arctic Ocean (Maxwell, 1981). The frequency of westerly winds  $\geq 40$  km/hr reaches 15-20% (Jan) and 5-10% (July) as compared to 4% and 2%, respectively, for Eureka (Maxwell, 1981). In E Norwegian Bay, 30% of recorded wind trajectories (Aug-Sept) were from the west, 2% of which exceeded 87 km/hr (Fisheries and Environment Canada, 1978). The incursion of westerly winds produces higher precipitation compared with Nansen and Eureka sounds. Annual precipitation ranges from 100-125 mm (35-40% as rain) compared to <100 mm for Eureka (Maxwell, 1981). This is accompanied by an increase in the frequency of summer fog and low cloud. However, mean annual temperature range is still high (40° C; Maxwell, 1981). During the six week field season in 1997, precipitation and fog attained a 75% frequency.

The regional equilibrium line altitude (ELA) and glaciation level (GL) in Baumann Fiord also reflect the influence of Norwegian Bay on the climatic regime of SW Ellesmere Island. Glaciation levels surrounding Baumann Fiord range from 600-800 m asl, compared to 800-1100 m asl at sites further north (Miller *et al.*, 1975). England (1986) proposed that the palaeoglaciation level in inner Greely Fiord (presently 900 m asl; Figure 1.2) decreased to at least 475 m asl during the last glaciation. Hodgson (1985) also proposed that local ice caps developed on the Braskeruds Plain (350-500 m asl) during the LGM.

The field area is presently unglaciated, and large, perennial snow patches discernible on air photos are rare. The Sydkap Ice Cap (65 km<sup>2</sup>) lies 35 km to the south. This ice cap has a maximum surface elevation of 1490 m asl (Canadian Topographic Service, 1975). The range in ELA of 400 to >800 m asl on the Sydkap Ice Cap declines steeply to the south (Miller *et al.*, 1975). Mass balance measurements on the Prince of Wales Icefield also show a similar regional gradient (Koerner, 1979). Accumulation

exhibits a 50% *decrease* on the west side of the icefield within 2 km of the crest (Koerner, 1979). Consequently, ice on the east side of the Prince of Wales Icefield is significantly thicker than that on the west. The overall preferential accumulation on SE Ellesmere Island relates to greater snow accumulation due to the proximity of the North Water polynya in N Baffin Bay (Miller *et al.*, 1975; Koerner, 1979). Reeh (1984) suggested that the asymmetry of ice caps in E. Ellesmere Island may have been equally pronounced during glacial times.

# CHAPTER TWO

## 2.1 Introduction

Reconstruction of the glacial and sea level history of central Baumann Fiord involved the investigation of glacial and marine sediments and their associated landforms. The techniques described in this chapter are presented in the order in which they fulfill the research objectives.

Firstly, the surficial sediments and associated landforms of central Baumann Fiord have been interpreted by air photo and field mapping. Secondly, raised marine sediments and associated landforms have been surveyed, described, and when appropriate, dated. Radiocarbon age determinations on raised marine sediments provide the chronological control for deglaciation in central Baumann Fiord.

## 2.2 Research Methods

### 2.2.1 *Surficial Mapping*

Preliminary identification of glacial sediments and landforms on E Svendsen Peninsula, Hoved Island and S Bjorne Peninsula was facilitated by air photo analysis, prior to departure into the field. From this analysis, sediments and landforms best suited to fulfill the research objectives were selected for field investigation. Surficial sediments are classified on the basis of morphology, texture and thickness, and are divided into six genetic units; (1) rock and residuum, (2) till, (3) glaciofluvial sediments, (4) raised marine sediments, (5) alluvium, and (6) colluvium (cf., Dyke, 1983). A brief overview of each unit and associated landforms is presented in this chapter. A detailed description is reserved for Chapter Three.

Exposures of bedrock, and surficial units comprised of *in situ* weathered bedrock byproducts were mapped as rock and residuum, respectively.

The extent and thickness of till was mapped principally by air photo analysis. Throughout the field area, till is subdivided into two units: blanket and veneer (Dyke, 1983). Till blankets exceed 2 m thickness, with the result that they completely obscure the underlying bedrock structure. Till veneer is of insufficient thickness (<2 m) to



completely conceal bedrock structure, and may consist only of sparse erratics amongst residuum. Till thickness determinations from aerial photographs utilize the distribution of ice-wedge polygons. These are helpful in identifying till blankets, because ice wedges are unable to form in sediments <2 m thick (Dyke, 1983). Till characteristics were further established by field mapping along three transects in each field area. These involved: (1) a 30 km long, E-W transect from the mouth of Vendom Fiord to the highlands east of Svarte Fiord, (2) a reconnaissance survey of Hoved Island, and (3) a 50 km transect from the west coast of Sor Fiord to the head of Eids Fiord, across the base of Bjorne Peninsula (Figure 1.5). The distribution of granites throughout the field area is consistent with the westward advance of the Prince of Wales Icefield (cf., Hodgson, 1985; Bell, 1992; Ó Cofaigh, 1997, 1998b). Part of this thesis represents a preliminary investigation of granite mineralogy in order to determine till provenance. Two granite erratics collected from till samples on Hoved Island and S Bjorne Peninsula have been thin sectioned by D. Resultay (Department of Earth and Atmospheric Sciences, University of Alberta). I have examined each thin section with a petrographic microscope, and with the assistance of Dr. T. Chacko (Department of Earth and Atmospheric Sciences, University of Alberta) determined their texture, structure and mineralogy. These samples have been classified, and related to likely source areas, according to detailed lithological descriptions of the Precambrian Shield on the eastern QEI (cf., Frisch, 1988). Striae were recorded on aerial photographs and topographic maps, from which their orientation was determined.

Alluvial sands and gravels are divided into two types: deposits that are flooded every year (active), and those that are not (inactive). Active fluvial sediments have surfaces that are characteristically unoxidized and seasonally modified by channels fed by water during nival floods or summer storms. Inactive sediments generally have oxidized surfaces and are separated from the contemporary floodplain by a distinct escarpment  $\geq 1$  m high.

Raised marine sediments are categorized as deltaic, nearshore and beach deposits. Stratigraphic sections observed within raised marine sediments were recorded and interpreted using standard stratigraphic techniques, including unit texture, structure, thickness, lithology and mollusc species content (cf., Stewart, 1991). Stratigraphic descriptions are limited predominantly to deltas that have been dissected during postglacial emergence.

Moraines, kames and lateral meltwater channels were mapped, with emphasis on defining former ice margins and relating these to datable raised marine sediments.

Mapping lateral meltwater channels, by far the most abundant glacial landform observed in the field area, provides the principal method for delineating these ice margins. Lateral meltwater channels form because cold-based glaciers preclude effective drainage of supraglacial meltwater to subglacial pathways. Consequently, water flows across the glacier surface, and becomes concentrated at its margin. The resulting glaciofluvial channels delineate numerous, successive ice-marginal positions, nested in the direction of ice retreat. During optimal conditions for channel development, they may record ice-marginal retreat with annual resolution (Dyke, 1993).

Many of the ice-marginal landforms around central Baumann Fiord grade into sediments deposited as glaciers retreated in contact with the sea, which commonly contain datable marine fauna. In order to reconstruct the deglacial and sea level history of central Baumann Fiord, these sediments were related to former shorelines, and surveyed by micro-altimetry. The chronology of ice retreat and sea level change in central Baumann Fiord was provided by radiocarbon analysis of marine shells recovered from these sediments, which is discussed in the following section.

### *2.2.2 Establishing the elevation and age of former sea levels*

Part of this thesis represents an extension of the database on postglacial emergence constructed by others from research throughout Eureka Sound (Hodgson, 1985, 1989; England, 1990, 1992; Bell, 1996; Ó Cofaigh, 1998a and c; Bednarski, 1995, 1998; England and Ó Cofaigh, 1998). This work is concerned with delineating areas of former maximum ice sheet thickness, recorded primarily by the elevation and age of Holocene marine limit. Marine limit represents the maximum elevation attained by the sea along a formerly glacioisostatically-depressed coastline. Using the elevation and age of Holocene marine limit as a proxy for relative ice sheet thickness assumes that its elevation relates to a glacioisostatic adjustment that is proportional to ice sheet thickness during the LGM. Unfortunately, not enough data points were obtained during this research to construct relative sea level curves for central Baumann Fiord. Nevertheless, data presented in this thesis contribute new details to regional isobase maps.

Accurate reconstructions of postglacial emergence rely on the careful interpretation of raised marine landforms, and a proper identification of marine limit (Andrews, 1970). Problems may arise if a lower shoreline is misattributed to marine limit. For example, the establishment of marine limit may coincide with a period of low sediment input, producing an inconspicuous landform which may remain unrecognized.

Deposition into a subsequently lower sea level during a period of higher sediment input may create the misleading impression that this sea level represents true marine limit. Another problem may occur if marine landforms have experienced reworking during postglacial time. However, these problems can be minimized by using a variety of local landforms to determine marine limit (Andrews, 1970).

In order to establish the age of marine limit, it is important to attribute correctly a specific dated shell sample to its former sea level (Andrews, 1970). Shells collected from deltaic topsets are preferable, because they relate to the mean sea level at the time of deposition, although in some instances, delatic foresets can be traced to contemporaneous topsets. Shells recovered from stratigraphically-isolated nearshore or deep-water sediments relate to former sea levels an unknown elevation above the sample site. Therefore, these radiocarbon age determinations represent minimum age estimates for the establishment of marine limit.

In central Baumann Fiord, marine limit has been determined by measuring the elevation of raised strandlines, washing limits and the outer lip of well-preserved deltas. Elevations were determined using a Wallace and Tiernan barometric altimeter, which has an accuracy of  $\pm 2$  m at 100 m asl. Because altimeter readings are controlled by changes in temperature and atmospheric pressure, corrections for both have been made for each reading. Temperature was recorded during each altimeter reading, from which variations in elevation were quantified by standard temperature correction equations. Changes in atmospheric pressure were recorded by a micro-barograph located at camp. Because a systematic relationship exists between altimeter readings and changes in atmospheric pressure, barometrically-induced changes in altimeter data could be quantified and incorporated into the elevation calculations for each site. Local tidal range, indicated by the difference between sea level and the highest ice foot (cf., Blake, 1992) was less than 0.5 m. Therefore, elevation errors caused by tidal range are considered to be minimal. In all cases, the position of high tide was used as the datum. The accuracy of the altimetry could be assessed by noting the difference between the corrected elevation of camp at the beginning and end of each survey. In all cases, elevation variations were within the accuracy of the instrument ( $\pm 2$  m).

The age of marine limit was established by  $^{14}\text{C}$  dating marine shells collected from deltas, beaches and fine-grained nearshore sediment. The collection of paired valves found in growth position is always preferable; however, in some landforms, only fragments were present. When fragments were found, only an individual piece was submitted for radiocarbon dating, because multiple shell fragments may consist of a

range of ages. Although surface samples are less preferable, they are nevertheless useful for dating beaches close to marine limit. All shell samples recovered were placed in sterile plastic bags for their return to the laboratory.

The accuracy of  $^{14}\text{C}$  dating is entirely dependent on the quality of the shells submitted. Therefore, only shells that were free of surface pittings and visual contaminants were used. This is necessary because surface contaminants such as secondary calcite and organic encrustations will have different ages than the shell being dated and therefore need to be removed. Cleaning involved immersing shell samples in an ultrasonic bath of deionised water for 20 minutes in order to remove the fine-grained sediment from which the shells were recovered. After air drying, each shell was cleaned with a small electric sander and a hand pick. The immersion process was repeated to remove any remaining abraded material. These samples were weighed, sealed in sterile bags and submitted to Beta Analytic Incorporated (Miami) for radiocarbon analysis. Two samples weighing >30 g were dated using conventional radiocarbon analysis (beta counting) and three smaller samples (4-6 g) were dated using accelerator mass spectrometry (AMS) on individual fragments (not the entire sample). The radiocarbon ages of these samples have been converted into calendar years using radiocarbon calibration program REV 3.0 (Stuiver and Reimer, 1993). The results of this analysis are presented and discussed in Chapter Four.

Collectively, these data have been used to determine the distribution, elevation and age of raised marine landforms throughout the study area. This provides the chronological control necessary to reconstruct deglacial activity and to determine the magnitude of postglacial emergence in central Baumann Fiord.

## CHAPTER THREE

### 3.1 Introduction

Mapping the surficial geology and geomorphology, coupled with radiocarbon dating of fossil marine molluscs were the principal methods used to reconstruct the Late Quaternary glacial and sea level history of Svendsen Peninsula, Hoved Island and Bjorne Peninsula. Surficial sediments are divided into six genetic units, according to Dyke (1983). These units are presented in the following sections, based on their relative age, from oldest to youngest. Discussion of the relevance of these units to the reconstruction of the Late Quaternary glacial and sea level history of central Baumann Fiord is reserved for Chapter Four.

### 3.2 Rock and Residuum

Rock and weathered rock (residuum) constitute a widespread surficial unit on E Svendsen Peninsula and Hoved Island, whereas on S Bjorne Peninsula, their distribution is more restricted (Figure 3.1).

The highland ridges of E Svendsen Peninsula are dominated by oxidized, pitted bedrock (sandy limestone) that has undergone frost shattering, producing extensive blockfields. Shattered and pitted surfaces of sandy limestone also extend upslope from Holocene marine limit, west of the mouth of Svarte Fiord. This contrasts with the subdued relief that dominates the lowland terrain of E Svendsen Peninsula, where unweathered dolomitic limestone is exposed on the banks of rivers, which incise the gently undulating lowlands (Figure 3.2)

Surveys of Hoved Island reveal carbonate ridges of moderate relief surrounded by blockfields. Elsewhere, sandy limestone blocks display granular disintegration, producing extensive *grus* veneers. The lowland terrain that divides these ridges consists predominantly of fine grained carbonate residuum, and discontinuous till veneer (Figure 3.1).

On S Bjorne Peninsula, sandy limestone outcrops in the highlands that flank the south coast of Baumann Fiord, as well as the uplands west of Sor Fiord (Figure 3.1). Tabular blocks of oxidized, pitted sandy limestone throughout these highlands testify to

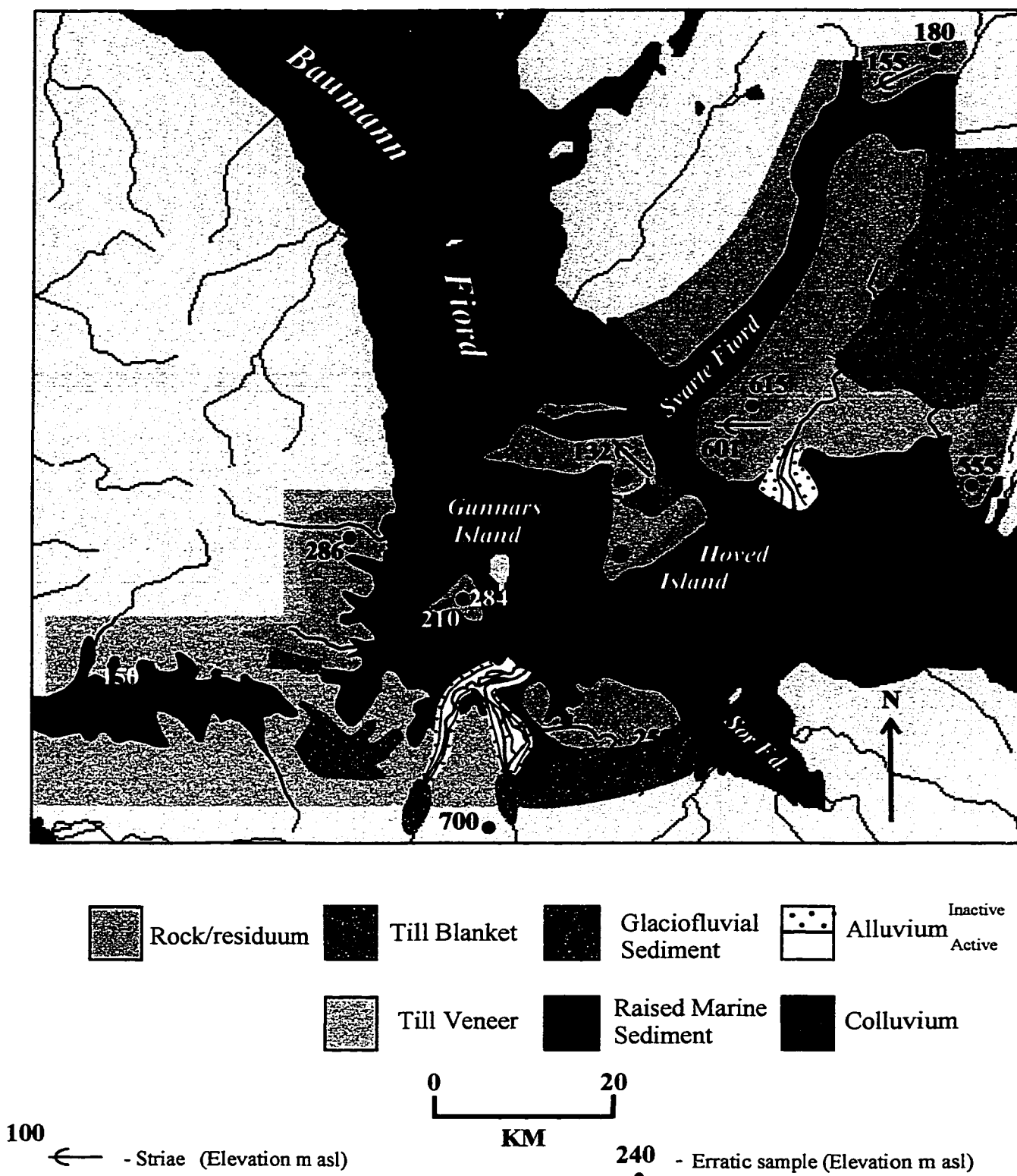


Figure 3.1 Eastern Svendsen Peninsula, Hoved Island and southern Bjorne Peninsula showing the distribution of the surficial sediments and glacial landforms cited in text

the effectiveness of frost shattering in the field area. Outcrops of dolomitic limestone and calcareous shale are exposed on river banks. Bioclastic limestone outcrops as linear tors in south-central Bjorne Peninsula, parallel to the axis of the Schei Syncline. Granular disintegration of these tors has produced non-sorted stripes, which mantle the undulating lowlands. Large areas of carbonate bedrock show no evidence of glacial erosion, although granite erratics lie scattered on the surfaces of bedrock and residuum in all parts of the field area. A description of the texture, structure and mineralogy of such granites, and a discussion of their provenance is presented in Section 3.3.1.

### 3.2.1 *Associated Landforms*

Because of the susceptibility of carbonate bedrock to solution weathering, examples of glacial erosion preserved on it are rare. However, on the highlands of E Svendsen Peninsula, a striated surface (20 cm<sup>2</sup>) of sandy limestone was observed at 601 m asl (Figure 3.1). This surface displays poorly preserved striae orientated 270°, which relate to the westward flow of ice, parallel to inner Baumann Fiord, across the highest structural grain. On Hoved Island, a patch (60 x 40 cm) of abraded sandy limestone at 132 m asl exhibits conspicuous striae orientated 316° (Figures 3.1 and 3.3). These record ice-flow to the NW, nearly parallel to the axis of outer Baumann Fiord. At the head of Svarte Fiord, NE-SW trending exposures of dolomitic limestone have been streamlined by a glacier flowing orthogonally across them. Up-glacier surfaces of these bedforms exhibit well-preserved striae at 155 m asl, orientated 237° (Figure 3.1). These striae suggest that Svarte Fiord was an outlet for glaciers flowing from the NE, across Svendsen Peninsula.

## 3.3 Till

Discontinuous till *veneer* describes scattered erratics resting on bedrock or residuum (Figure 3.4). Although the surface of this unit often reflects the composition of the underlying bedrock, and is texturally similar to residuum, it is categorized as till, on the basis of its erratic content. Till veneer, containing occasional faceted granite boulders and cobbles, is the most widespread till unit mapped from the mouth of Vendom Fiord to the east coast of Svarte Fiord (Figure 3.1). On level ground, the surface of this till exhibits cryoturbation, indicated by low relief (<10 cm) mudboils containing fragments of dolomite within the fine-grained calcareous matrix. Vegetation

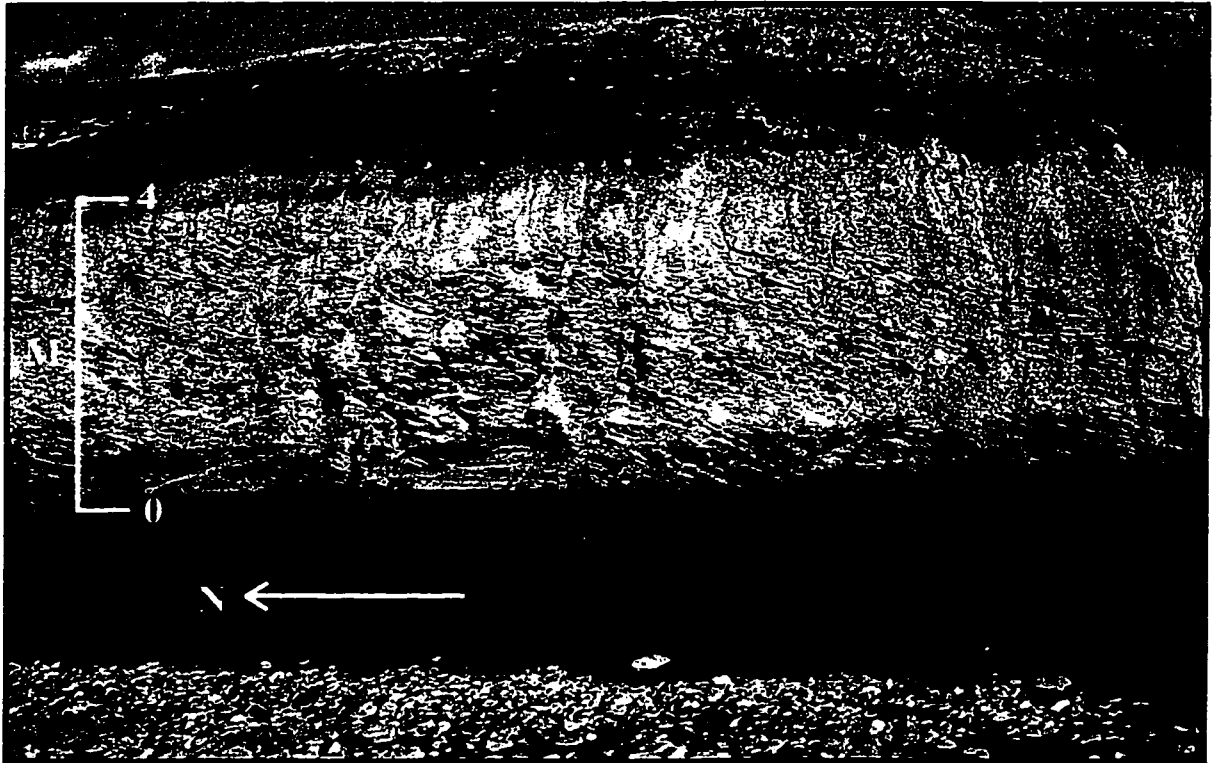


Figure 3.2. Unweathered dolomitic limestone overlain  
by till veneer on eastern Svendsen Peninsula



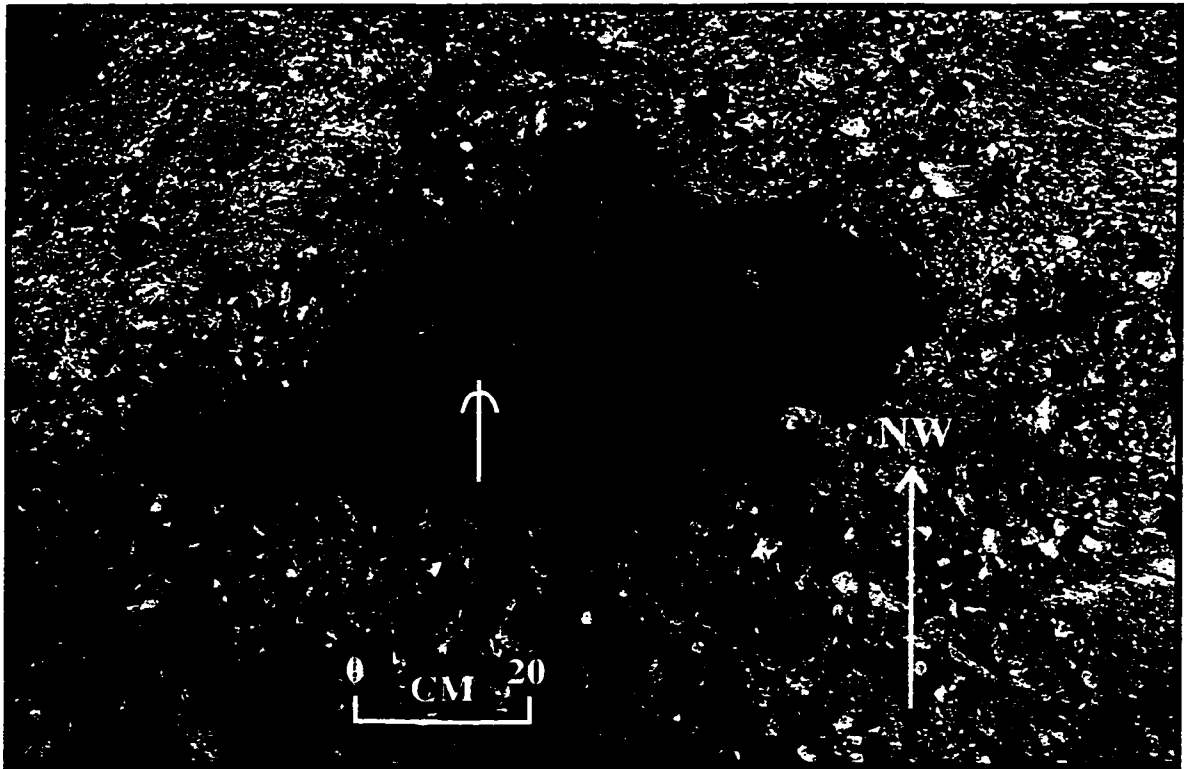


Figure 3.3. Northwest trending striae abraded into an exposure of sandy limestone on Hoved Island

is restricted to small depressions and gullies, where there is increased moisture. Moreover, the distribution of vegetation may also indicate that nutrients supporting plant growth are deficient within the till veneer, which likely reflects a paucity of shield-derived material, particularly the weathering products of feldspar (Dyke, 1983). An increase in the distribution of vegetated till (>50% ground cover; Dyke, 1983) exhibiting dense networks of polygons in the northern part of the E Svendsen Peninsula indicates an increase in both till thickness and granite content. Therefore, this unit is mapped as till *blanket* (Figure 3.1). Well-rounded, boulder-sized granite erratics were also examined on the highland ridges of E Svendsen Peninsula, up to 615 m asl (Figures 3.1 and 3.5). Furthermore, granite erratics mantle all of the terrain examined on Hoved Island, up to 300 m asl (Figure 3.1).

On SE and south-central Bjorne Peninsula, till surfaces exhibit dense networks of low-centre, non-sorted polygons (up to 1 m in diameter) on more level ground, and closely spaced, non-sorted stripes on slopes. This area is commonly well vegetated, and is mapped as till blanket (Figure 3.1). A reduction in the extent of polygonization and vegetation cover (defined by lighter tones on air photos) on units in south-central and SW Bjorne Peninsula are inferred to record a decrease in till thickness and granite content. Therefore, this unit is mapped as till veneer (Figure 3.1). The surface of this till veneer is generally featureless, and is characterized by poorly sorted mudboils with moderate-relief ( $\leq 30$  cm).

Till veneers and blankets mapped across S Bjorne Peninsula, from the west coast of Sor Fiord to the head of Eids Fiord contain granite erratics ranging from well-rounded pebbles to angular boulders ( $2 \text{ m}^3$ ; Figure 3.6). High elevation granite boulders, and a small patch of granitic, shelly till were surveyed on the highlands that flank the south coast of central Baumann Fiord, at 286 and 210 m asl, respectively (Figures 3.1 and 3.7). However, the abundance of these erratics decreases southwards, towards Schei Syncline. Only one granite granule was observed on these highlands, at  $\sim 700$  m asl (J. England, personal communication, 1998; Figure 3.1). In addition to granite erratics, carbonate erratics occur throughout the field area. These increase in abundance towards Schei Syncline, and include three large bioclastic limestone erratics (up to  $3 \text{ m}^3$ ) grouped together in south-central Bjorne Peninsula, 20 km north of the Sydkap Ice Cap (Figure 3.8).

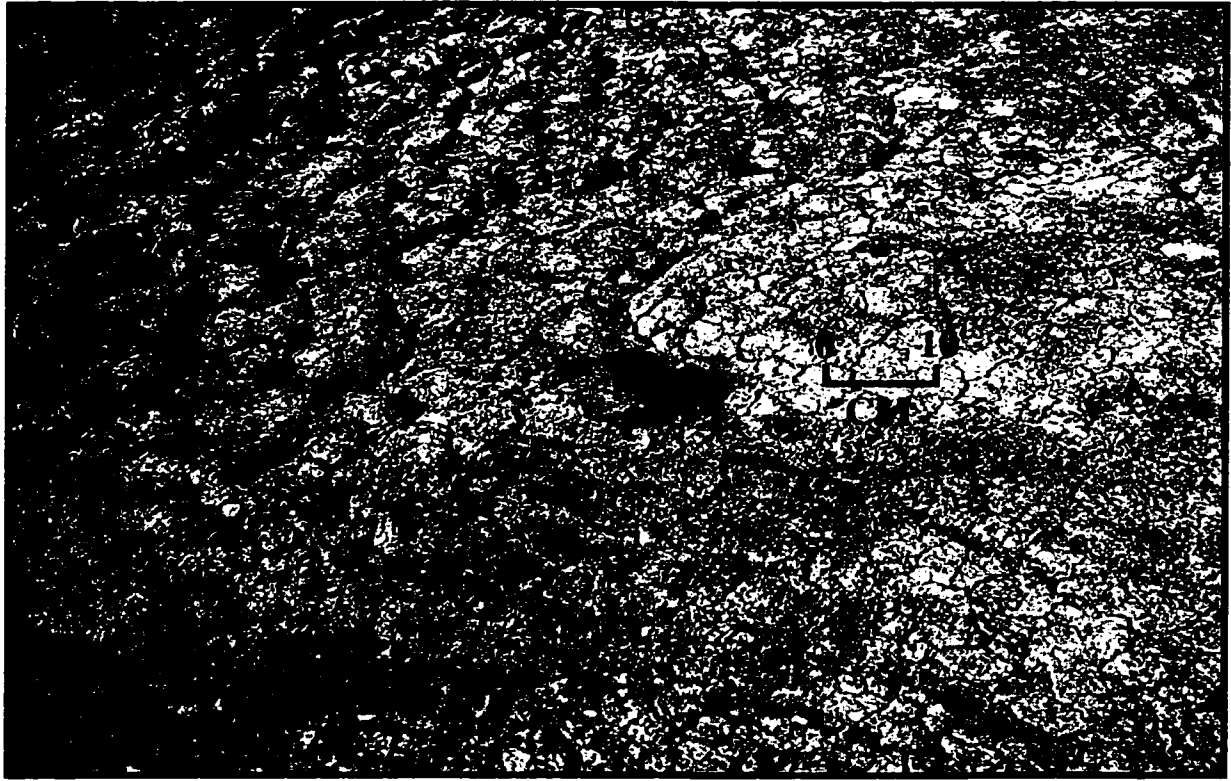


Figure 3.4. Surface of till veneer on eastern Svendsen Peninsula, showing conspicuous granite erratic



Figure 3.5. Granite erratic in sandy limestone blockfield at 615m asl, on the highlands of eastern Svendsen Peninsula

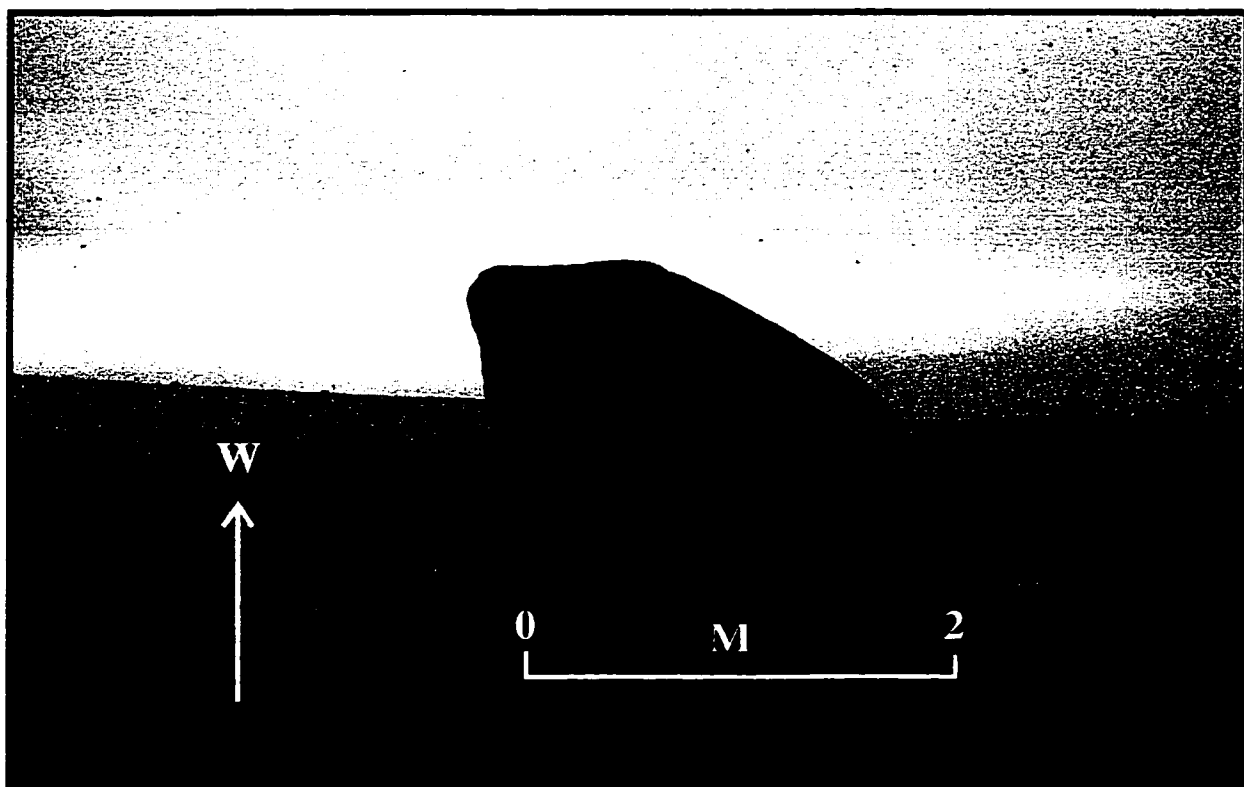


Figure 3.6. Granite erratic (150 m asl) at the head of Eids Fiord



Figure 3.7. Granite erratic in till blanket, at 284 m asl  
on the highlands of southern Bjorne Peninsula

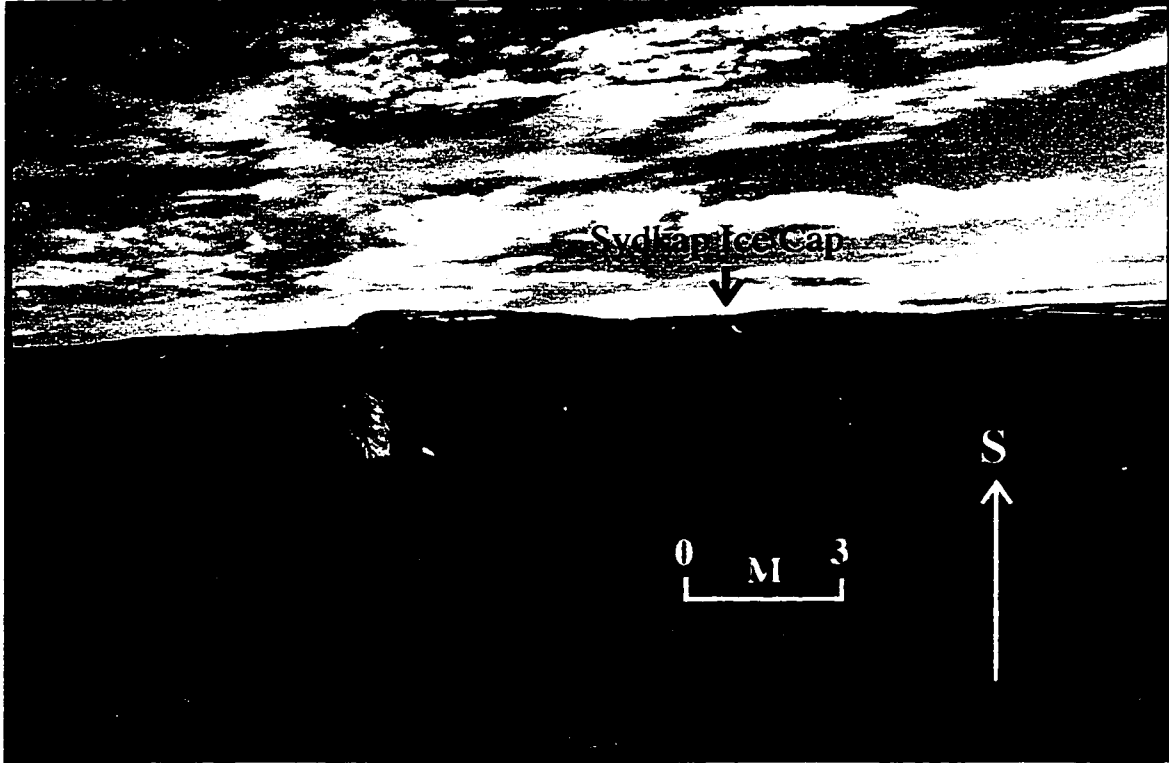


Figure 3.8. Three bioclastic limestone erratics grouped together on south-central Bjorne Peninsula, 20 km north of the Sydkap Ice Cap

### 3.3.1 *Provenance of erratics*

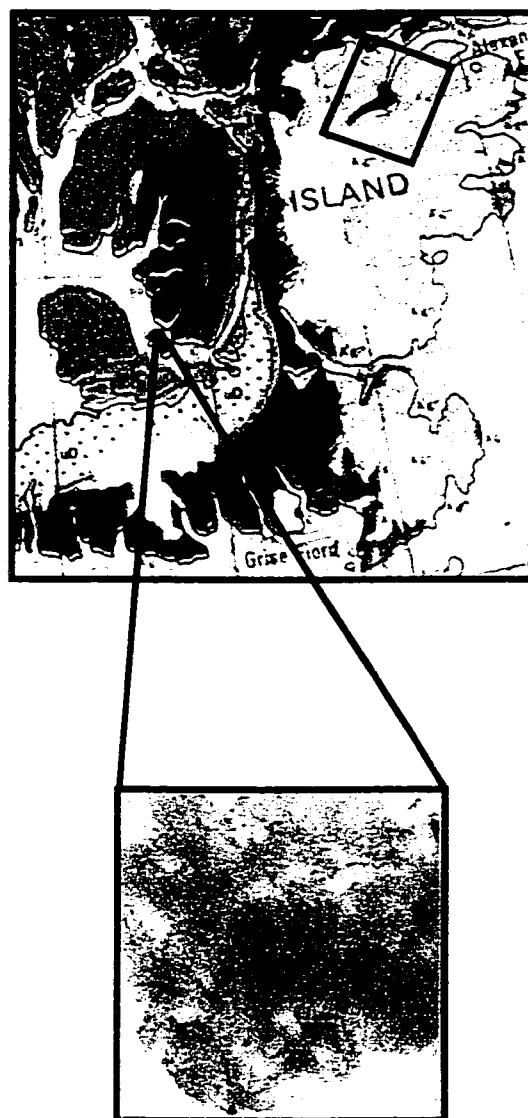
Granite erratics examined on E Svendsen Peninsula and Hoved Island consist of medium-grained, pink to red, felsic varieties (Figures 3.4 and 3.5). Thin section analysis of a granite from Hoved Island (provided by R. Smith, University of Alberta) reveals a dominance of alkali feldspar and quartz (Figure 3.9). Examples of garnet, exhibiting poor crystal habit, are sparsely distributed within the thin section. According to texture and mineralogy, and the presence of weak gneissic layering, I have identified this sample as anatectic biotite granite (unit ag; Frisch, 1988). This distinctive variety of granite occurs throughout the crystalline terrain of east-central Ellesmere Island (Figure 1.3). It is particularly abundant in Makinson Inlet and Baird Inlet, and east and west of Jokel Fiord (Figure 3.9; Frisch, 1988).

Granite erratics examined in till on S Bjerne Peninsula also consist of medium-grained, pink to red varieties (Figure 3.7). Thin section analysis of a granite cobble collected at 250 m asl from the uplands of SE Bjerne Peninsula contains alkali feldspar, quartz and sufficient quantities of biotite to impart well developed gneissic banding (Figure 3.10). Green spinel is distributed intermittently within the thin section (T. Chacko, personal communication, 1998). This sample is distinguished from the granite described from Hoved Island by the presence of layers and schlieren, which are related to the orientation of biotite sheets. According to these characteristics, I have identified this sample as layered anatectic biotite granite (agl) which is particularly abundant around Makinson Inlet (Figure 3.10; Frisch, 1988), somewhat further south than the proposed source for the granite sampled on Hoved Island. Both varieties of anatectic biotite granite (ag and agl) are mineralogically distinct from the crystalline terrains of S Ellesmere Island and Devon Island, which are characterized by orthopyroxene-bearing granite and gneiss, respectively (Frisch, 1988). Bioclastic limestone erratics on S Bjerne Peninsula likely relate to the Blue Fiord Formation, which outcrops in the Schei Syncline.

### 3.3.2 *Associated Landforms*

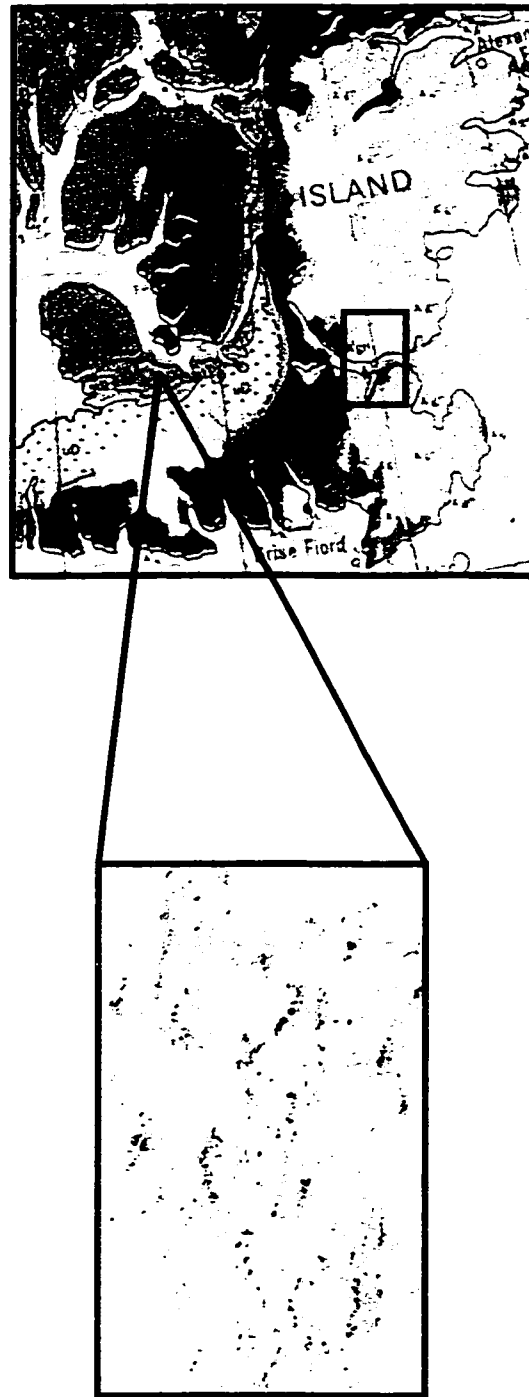
Glacial depositional landforms, particularly those relating to trunk ice inundating Baumann Fiord, are rare in the field area. Deglacial landforms that contact raised marine sediments provide important information regarding the style and chronology of ice-





x 1.5 actual scale

Figure 3.9. Thin section of anatectic biotite granite from Hoved Island, showing possible source area (boxed, Geological Survey of Canada, 1970)



x 1.5 actual scale

Figure 3.10. Thin section of layered anatectic biotite granite from southern Bjorne Peninsula, showing possible source area (boxed; Geological Survey of Canada, 1970)

retreat, from marine to terrestrial margins. Therefore, a description of these landforms is reserved for Chapter Four.

### 3.4 Glaciofluvial Sediments and Landforms

Glaciofluvial sand and gravel constitutes a small proportion of the mappable sediment in the field area. Two valley trains, composed of limestone and occasional granite boulders, occur on the ice-distal (northern) side of the Schei Syncline (Figure 3.1). These narrow tracts of proglacial outwash are attributed to the southward retreat of the Sydkap Ice Cap, along river valleys that incise the Schei Syncline. Palaeochannels are preserved on oxidized outwash terraces (inactive alluvium), 1-5 m above contemporary stream beds. The lower outwash surfaces (active alluvium) are dissected by braided streams, sustained by nival discharge from the surrounding highlands, and meltwater from the Sydkap Ice Cap. Proglacial outwash is inconspicuous in E Svendsen Peninsula, although meltwater channels are common. This may relate to the retreat of cold-based glaciers containing small amounts of debris (Ó Cofaigh, 1998a).

Because the style of terrestrial deglaciation in E Svendsen Peninsula and S Bjerne Peninsula is based primarily on the distribution of lateral meltwater channels, a description of these channels, and their associated raised marine sediments, (which provide deglacial chronology) is best developed in Chapter Four. Nonetheless, because lateral meltwater channels are the most abundant ice-marginal landform observed within the field area, it is important to refer to their association with the surficial sediments described in this chapter.

In the rock/residuum and till terrains of E Svendsen Peninsula and Svarte Fiord, closely-spaced sets of sub-parallel, low gradient, SW-trending lateral meltwater channels have been eroded from ~350 m asl to marine limit. The lowest channels terminate at Holocene raised marine sediments (Section 3.5). Collectively, these channels record a NE pattern of ice-retreat, towards the interior of Svendsen Peninsula.

In the rock/residuum and till terrains of S Bjerne Peninsula, closely-spaced sets of sub-parallel, low gradient, northward-trending lateral meltwater channels were observed from 270 m asl to marine limit. The lowest channels also terminate at Holocene marine sediments (Section 3.5). These channels record a southerly pattern of ice-retreat, towards the Sydkap Ice Cap.

A kame,  $\geq 3$  m high and 30 m long, containing well rounded, moderately well sorted limestone and granite cobbles and boulders occurs at ~120 m asl on the west

coast of Sor Fiord (Figure 1.5). A description of this kame, and a discussion of its significance to the deglaciation of central Baumann Fiord is presented in Chapter Four.

### 3.5 Raised Marine Sediments

The coast of the field area is mantled by marine sediments that transgressed the glacioisostatically-depressed shoreline of central Baumann Fiord during deglaciation. These sediments are confined to the coast of E Svendsen Peninsula, where they extend to 87 m asl (Holocene marine limit). This includes a strip ~2 km wide and 25 km long (Figure 3.1). Raised marine sediments are significantly more widespread on S Bjorne Peninsula, where ~50% of the peninsula lies below Holocene marine limit (Figure 3.1). The distribution of these sediments is discussed in the following section. Because raised marine landforms record the deglacial and sea level history of central Baumann Fiord, their stratigraphy, sedimentology and age are presented in detail in Chapter Four.

#### 3.5.1 *Deltaic, beach and nearshore sediments*

On E Svendsen Peninsula, examples of well-preserved deltas are confined to the western highlands, where they are associated with lateral meltwater channels that contact Holocene marine limit. However, small, well-preserved marine limit deltas are associated with lateral meltwater channels along the west coast of Svarte Fiord. These are composed of topset gravel and sand, foreset sand and bottomset sandy-silt.

Large deltaic accumulations of topset gravel and sand, foreset sand and bottomset sandy-silt occur on S Bjorne Peninsula. These are common at the foot of the Schei Syncline, where they are associated with lateral meltwater channels that contact Holocene marine limit (Figure 3.1). These deposits exhibit fluvial incision during postglacial emergence. However, the original morphology of the delta surface is adequately preserved for surveying and sample collection.

Nearshore sediments mantle the coastal plains of the field area (Figure 3.1). These consist of prodeltaic accumulations of fine sand and silt. The abundance of nearshore sediment in the field area, particularly on S Bjorne Peninsula, is interpreted to record the deposition of suspended sediment from retreating ice margins, concomitant with marine transgression. The nearshore sediments exhibit low-centre, rectangular polygons, and numerous, large, fine-grained mudboils (up to 50 cm wide, 25 cm high; Figure 3.11). The poor drainage created by the fine texture of the nearshore sediment

produces wet meadows, that are recognizable as dark-toned areas on air photos (cf., Dyke, 1983).

Raised beaches, represented by low-amplitude (<50 cm), long wavelength (up to 50 m) berms are well-preserved below Holocene marine limit. Berms are composed of fine to medium grained, angular calcareous gravel, reworked from local sources. The angularity of the gravel is interpreted to relate to sediments derived from subaerial weathering or till or bedrock. These extend for many kilometers along the coast of central Baumann Fiord, although their amplitude increases towards modern sea level. These characteristics may record increases in the rate of sedimentation and/or decreases in the rate of marine regression during glacioisostatic recovery in central Baumann Fiord. Coarse deltaic and beach sediments observed on E Svendsen Peninsula and S Bjorne Peninsula show little evidence of cryoturbation.

### 3.6 Alluvium

Most of the alluvium mapped on E Svendsen Peninsula occurs as a 4 km<sup>2</sup> sandur (Figure 3.1). The sandur is divided into active and inactive surfaces. Twenty five percent of the sandur surface consists of sand and boulder gravel contained within a 4 km long, 800 m wide channel that bisects the sandur. This represents the active flood zone, which contains braided channels, individually  $\geq 10$  m wide. The remaining sand and gravel in the sandur is categorized as inactive alluvium. This occurs within a flight of four paired terraces, on either side of the active channel. The terraces become progressively wider as their elevations decrease towards modern sea level. All four terraces are dissected by braided palaeochannels, and they are separated from each other by a low ( $\leq 1$  m) escarpment. These terraces likely record increases in the rate of sediment progradation and/or decreases in the rate of marine regression during glacioisostatic recovery in central Baumann Fiord.

Contemporary sandy outwash, dissected by braided channels, individually  $\geq 20$  m wide, represents a significant portion of the alluvium mapped on S Bjorne Peninsula (Figure 3.1). Inactive alluvium (oxidized sand and silt) is contained within terraces  $\geq 3$  m above the margins of the active flood zone. These terraces are traversed by braided palaeochannels. The coarse, well-drained texture of the active and inactive alluvium explains the absence of cryoturbation on the terrace surfaces.

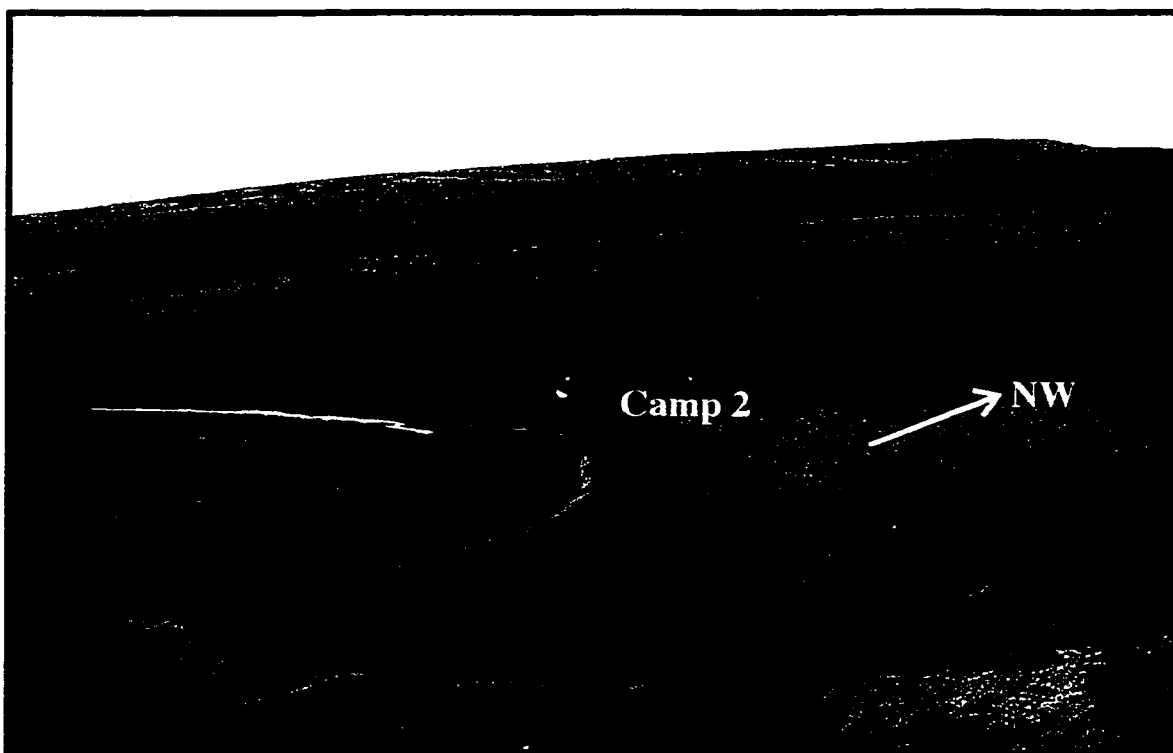


Figure 3.11. Rectangular polygons within fine-grained nearshore marine sediment on southern Bjorne Peninsula (camp for scale)

### 3.7 Colluvium

In the high-relief regions of E Svendsen Peninsula and S Bjorne Peninsula, many slopes are mantled by talus cones and colluvial aprons, derived from sandy limestone bedrock that has been frost shattered. However, the small aerial extent of the colluvium does not permit representation at the scale shown in Figure 3.1.

On the lowland terrain of E Svendsen Peninsula, colluvium extends downslope from the lowland surface, onto the 2 km wide coastal zone on the north shore of central Baumann Fiord (Figure 3.1). The colluvial aprons are commonly derived from downslope movement of the fine-grained till veneer that mantles the southern part of the lowland. This slope is traversed by numerous small streams, which remove the sediment transported to their courses by gelifluction and sheetwash.

Fine-grained colluvium represents a very small proportion of the surficial units mapped on the uplands of SE Bjorne Peninsula. This may be because many of the slopes are well vegetated, which likely contributes to increased slope stability and little exposure. In the lowlands of south-central Bjorne Peninsula, colluvial aprons are confined to river banks, where they are derived from the downslope movement of poorly vegetated till veneer, undercut by adjacent streams (Section 3.2).

### 3.8 Summary

This section summarizes the landforms and sediments that relate to the extent and configuration of former glaciers in central Baumann Fiord. The distribution of till, erratics and striae indicate that central Baumann Fiord has been inundated by ice, of sufficient thickness to envelop the entire field area, and override intervening highlands.

Medium-grained, pink to red varieties of granite distributed throughout the field area are interpreted to have originated from the crystalline terrain of E Ellesmere Island. However, the dispersal of some erratics could relate to Tertiary fluvial activity which deposited sediments over the former landscape of SW Ellesmere Island. Moreover, their distribution throughout the field area may not necessarily reflect their primary derivation (i.e., erratics could have been removed during previous glaciations and redistributed during the LGM). Consequently, determining glacier extent and regional ice-flow patterns solely according to the spatial distribution of granite erratics can be problematic. However, the distribution of faceted granite erratics *and* striae at the head of Svarte

Fiord strongly suggest that ice advanced towards Baumann Fiord as a result of a SW expansion of the Prince of Wales Icefield, across Svendsen Peninsula. This trajectory, which reflects a general topographic control of ice-flow is consistent with the LGM palaeogeography of west-central Ellesmere Island proposed by Ó Cofaigh (1998c), which shows regional (granite-carrying) ice flowing through Vendom Fiord (Figure 1.2). Therefore, striae on E Svendsen Peninsula and Hoved Island and anatectic biotite granite on Hoved Island which *may* have originated from Jokel Fiord/Baird Inlet, indicates that the SW expansion of the Prince of Wales Icefield extended at least as far as central Baumann Fiord. Ó Cofaigh (1998c) attributed the decrease in abundance of granite erratics west of the mouth of Trolld Fiord (Figure 1.2) to the outflow of local ice from Trolld Fiord, which deflected regional ice off-shore, into outer Baumann Fiord. Collectively, these data infer that Baumann Fiord was fully occupied by trunk ice during the LGM. The distribution of lateral meltwater channels on E Svendsen Peninsula indicates that the ice-retreat proceeded to the NE (the reverse of the advance pattern; cf., Bednarski, 1998).

Medium-grained, pink to red varieties of granite distributed throughout S Bjorne Peninsula are also interpreted to have originated from E Ellesmere Island. Although their abundance decreases southwards, towards Schei Syncline, they record an advance of the Prince of Wales Icefield, through Baumann Fiord, across Bjorne Peninsula towards Norwegian Bay. Layered anatectic granite identified on S Bjorne Peninsula *may* have been deposited by ice that flowed across Makinson Inlet. A southward increase in abundance of carbonate erratics towards Schei Syncline likely records the progressive influence of a northward expansion of the Sydkap Ice Cap, which presumably coalesced with regional ice flowing across Bjorne Peninsula. Ice-retreat patterns on S Bjorne Peninsula indicate that deglaciation proceeded towards the SE (to the Sydkap Ice Cap).

The next chapter addresses the chronology of this glacial inundation, deduced by its history of retreat, according to the distribution of radiocarbon-dated ice-contact marine sediments throughout the field area.



## CHAPTER FOUR

### 4.1 Introduction

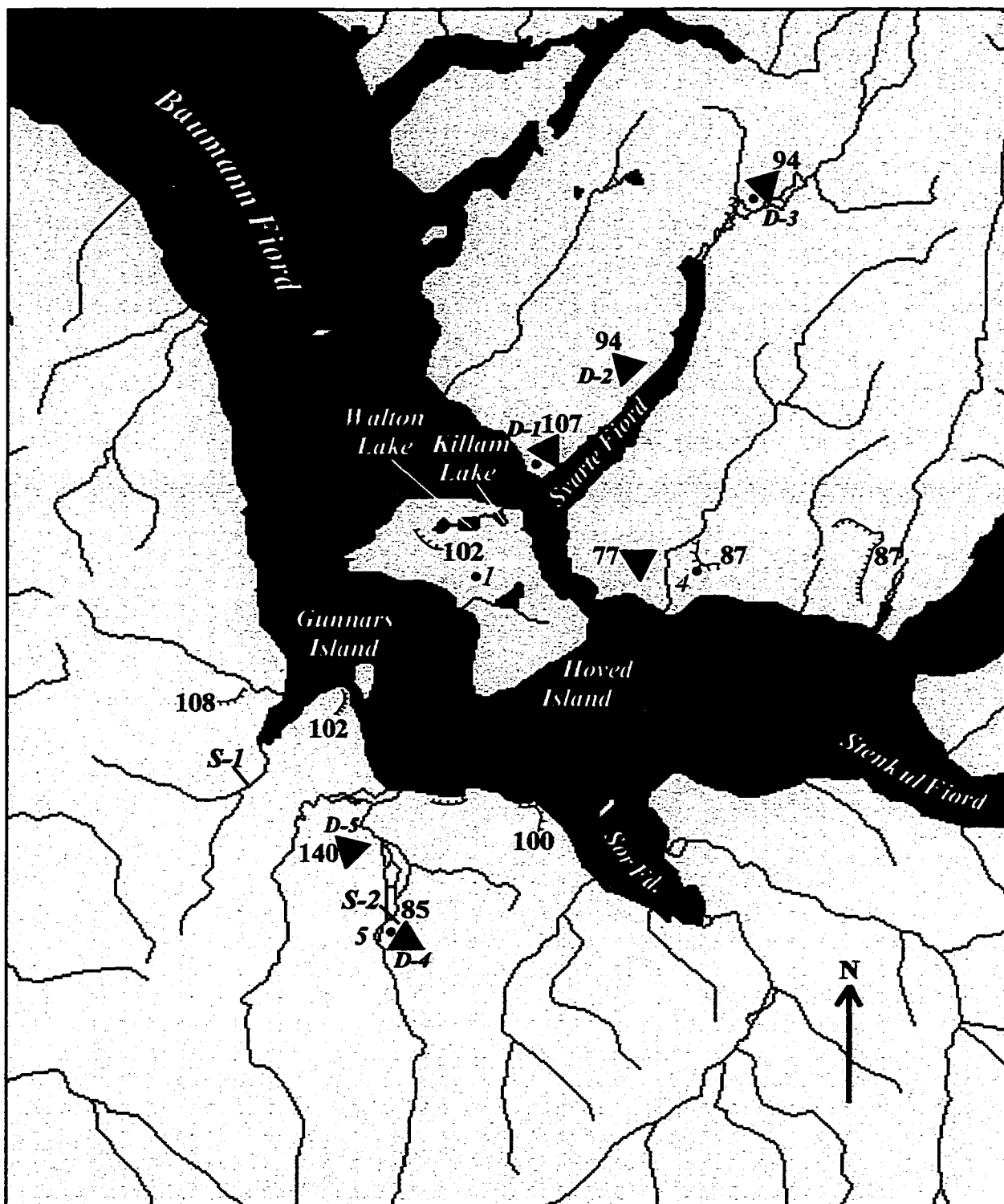
This chapter presents the chronology of deglaciation in central Baumann Fiord, based on ice-marginal landforms and raised marine sediments that record retreat from marine to terrestrial margins. The first section focuses on the style and chronology of deglaciation in Svarte Fiord and E Baumann Fiord. The second focuses on E Svendsen Peninsula and S Bjorne Peninsula.

### 4.2 Deglaciation in Svarte Fiord

A prominent delta at the mouth of Svarte Fiord marks marine limit at 107 m asl (*D-1*; Figure 4.1a). Because this deposit is perched against a sidewall of the inter-fiord highlands, and is without a modern sediment source, it must be ice-contact. Fragments of *Mya truncata* and *Hiatella arctica* recovered from coarse bottomset silt at 77 m asl dated  $8110 \pm 70$  BP (Beta 111678; Table 4.1). This date provides a minimum age for the initial re-entry of the sea which accompanied ice-retreat from outer Svarte and Baumann fiords (Figure 4.1a). Lateral meltwater channels were not observed along the outer coast of Svarte Fiord.

Lateral meltwater channels along the west coast of central Svarte Fiord (set A; Figure 4.1b) descend from ~140 m asl, across 15 km of weathered rock (residium), and contact a delta marking marine limit at 95 m asl (*D-2*; Figure 4.1a). Gelifluction obscures the delta front, so its stratigraphy (foreset and topset beds) was not observed. However, coarse silt, containing valves of *M. truncata* and *H. arctica* was exposed at the base of the delta. This sample has not been dated.

Well-developed sets of low-gradient (~7.5%) lateral meltwater channels also occur towards the head of Svarte Fiord (set B; Figure 4.1b). These are eroded into bedrock below ~250 m asl, and descend southwards for 2 km. Further inland, the head of Svarte Fiord bifurcates, producing north and northeast trending arms (Figures 1.6 and 4.1a and b). In the NE arm, an ice-contact delta records marine limit at 94 m asl (*D-3*; Figure 4.1a). A single fragment of *M. truncata* recovered from the bottomset silt at 88 m asl dated  $35,340 \pm 550$  BP (Beta 111704; Table 4.1). On the south side of the NE



*S-1* Sedimentary section

•  $^{14}\text{C}$  dated samples (1-5)

0 20  
KM

87 Marine limit elevation (m asl)

▲ - Delta surface

--- - Beach or washing limit

Figure 4.1a. Eastern Svendsen Peninsula, Hoved Island and southern Bjorne Peninsula showing marine limit elevations and distribution of radiocarbon-dated samples cited in text

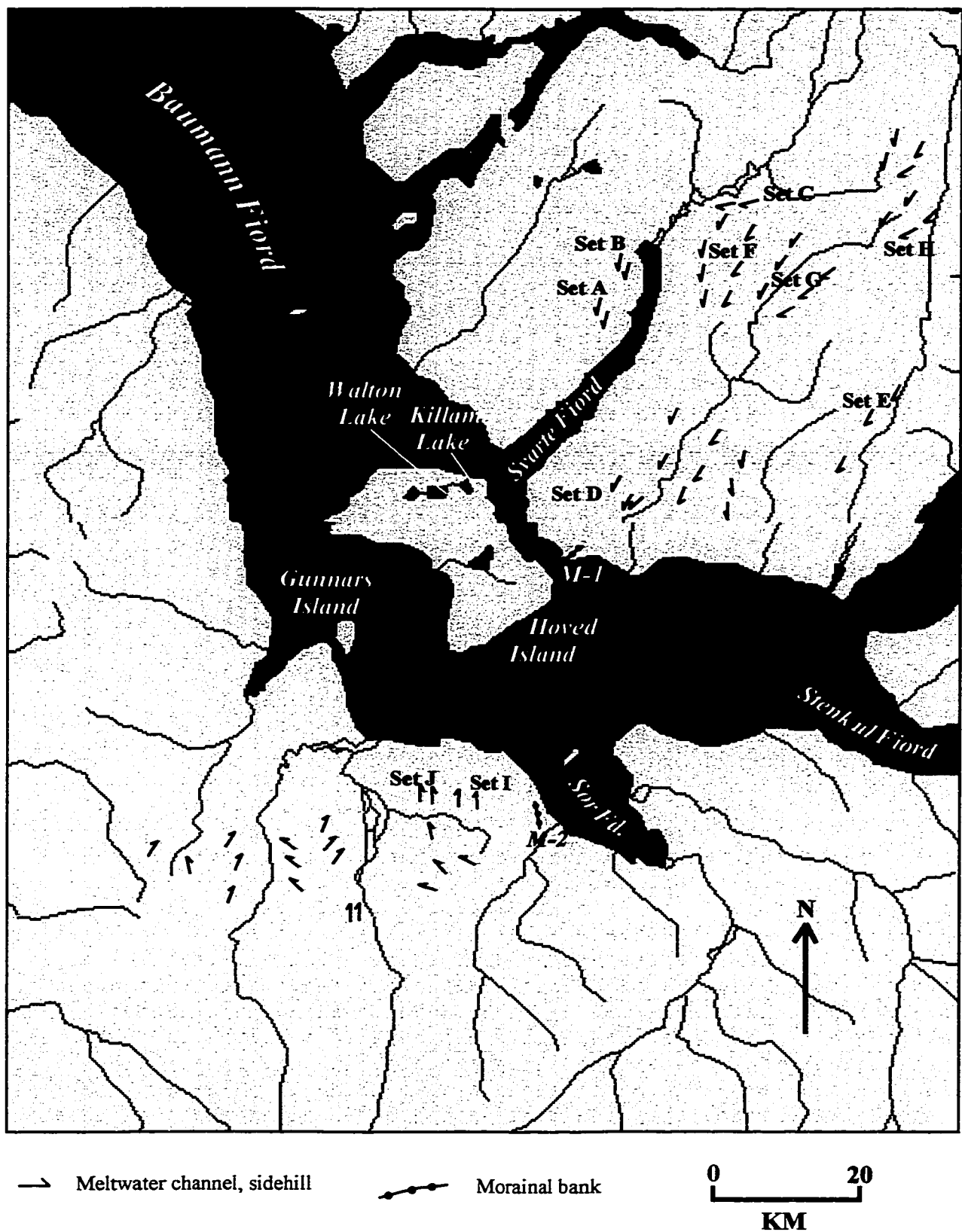


Figure 4.1b. Eastern Svendsen Peninsula, Hoved Island and southern Bjorne Peninsula showing deglacial landforms cited in text

**Table 4.1. Holocene radiocarbon dates, central Baumann Fjord**

Site	Location	Laboratory dating number	Material	Age (radiocarbon years BP) Conventional AMS	Calibrated Age (cal years BP)	Stratigraphy	Sample elevation (m asl)	Related RSL (m asl)
1	Hoved Island	Beta 111679	<i>M. truncata</i> and <i>H. arctica</i>	8000 +/- 70	8400	Marine silt	61	102
2	outer Svarte Fjord	Beta 111678	<i>M. truncata</i> and <i>H. arctica</i>	8110 +/- 70	8510	Bottomset silt	77	107
3	inner Svarte Fjord	Beta 111704	<i>M. truncata</i>	35 340 +/- 550	-	Bottomset silt	88	94
4	E. Svendsen Peninsula	Beta 111705	<i>M. truncata</i>	8380 +/- 100	8950	Marine silt	87	87
5	S. Bjorne Peninsula	Beta 111703	<i>H. arctica</i>	8050 +/- 70	8430	Forset sand	65	85

arm, well-developed sets of low-gradient (~10%) lateral meltwater channels are incised in bedrock below ~200 m asl, and descend SW for 1 km (set C Figure 4.1b). The similarity of Holocene marine limit recorded by deltas *D-2* and *D-3* (94 m asl; Figure 4.1) indicates a similar age (albeit undated).

## 4.3 Deglaciation in central Baumann Fiord

### 4.3.1 Eastern Svendsen Peninsula and Hoved Island

A sediment core (3 m thick) from Walton Lake, N Hoved Island (Figure 4.1a), contains two units (Smith, 1998). The basal unit consists of a 30 cm thick diamict containing angular carbonate clasts supported by a coarse-grained carbonate matrix. Granite clasts were not observed within the diamict, although they occur elsewhere on the island. The biological subfossil assemblage within the diamict consists of foraminifera, ostracods and paired molluscs. Paired valves of *Portlandia arctica* recovered from silt at the base of a 6 m core from Killam Lake (Figure 4.1a) indicate that glaciomarine sedimentation, and hence ice retreat from central Baumann Fiord, began  $\geq 9.3$  ka BP (Smith, 1998).

A sharp contact separates the second unit from the underlying diamict in Walton Lake. This consists of massive marine silt (2.7 m thick) containing rare dropstones. Paired valves of *P. arctica* recovered from this silt dated 8.6 ka BP (Smith, 1998). An isolated pocket of glaciomarine silt (with <10% dropstone content) was surveyed at 61 m asl on west-central Hoved Island ( $^{14}\text{C}$  sample 1; Figure 4.1a). This contains paired valves of *M. truncata* and *H. arctica* dated  $8000 \pm 70$  BP (Beta 111679; Table 4.1). Marine limit on Hoved Island is recorded by a gravel beach at 102 m asl (J. England, pers. comm., 1998; Figure 4.1a).

An elongate ridge extends into the narrow channel between E Svendsen Peninsula and S Hoved Island (*M-1*; Figures 4.1b and 4.2). The ridge is 2 km long, ~75 m wide, and displays an asymmetric profile, with steep up-fiord and gentle down-fiord slopes (Figure 4.3). An elevation of 55 m asl was recorded on its flat-topped, gravel surface. Unstratified marine silt at the base of the down-fiord slope contains paired valves of *H. arctica* at 48 m asl. This sample has not been dated.

Eight kilometers up-fiord from Killam Lake, till veneer is draped by marine silt. The upper limit of marine on-lap is interpreted to record marine limit at 87 m asl (Figure 4.1a). A single valve of *M. truncata* recovered from the surface of this deposit dated

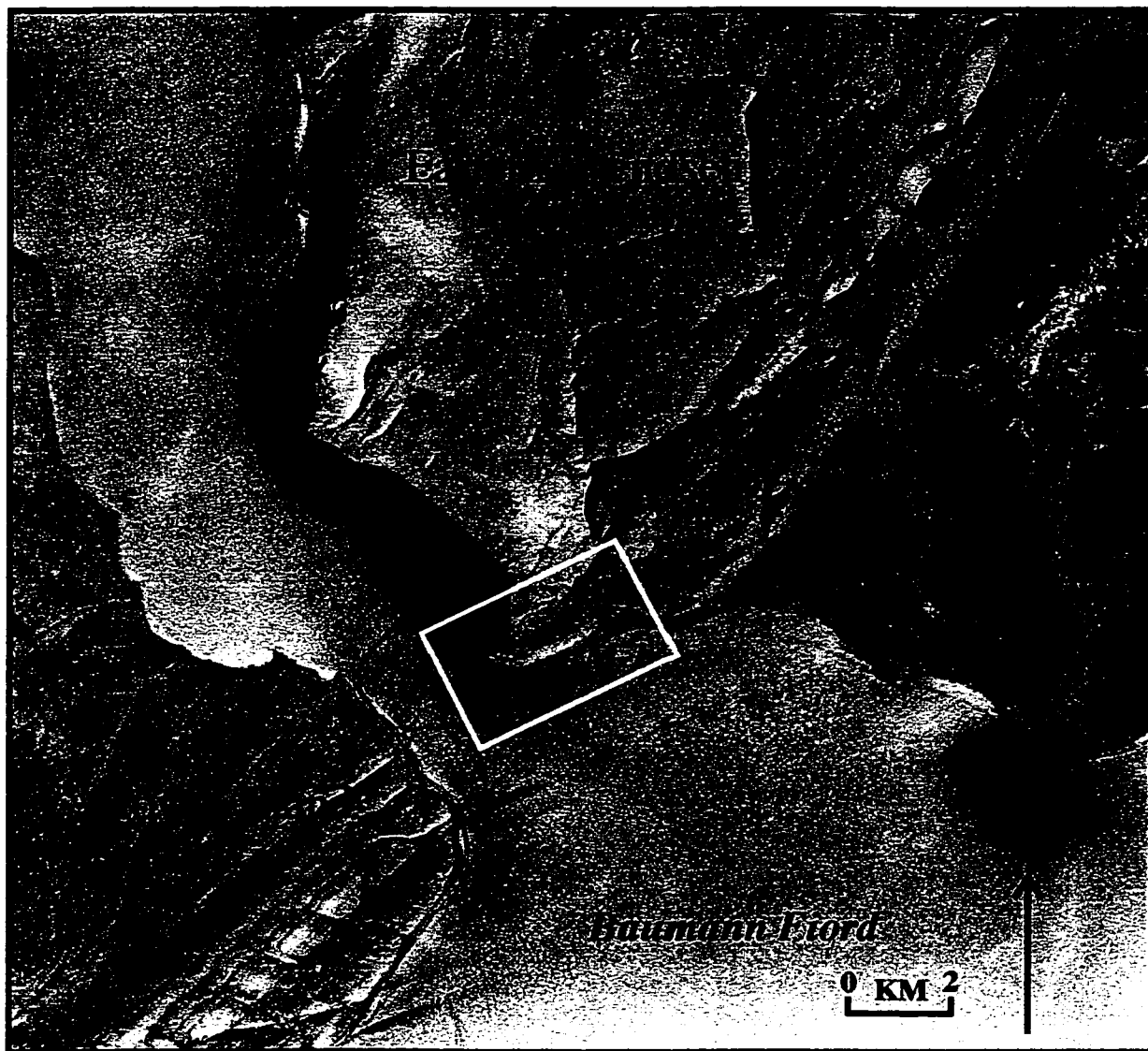


Figure 4.2. Location of *M-1* between eastern Svendsen Peninsula and Hoved Island

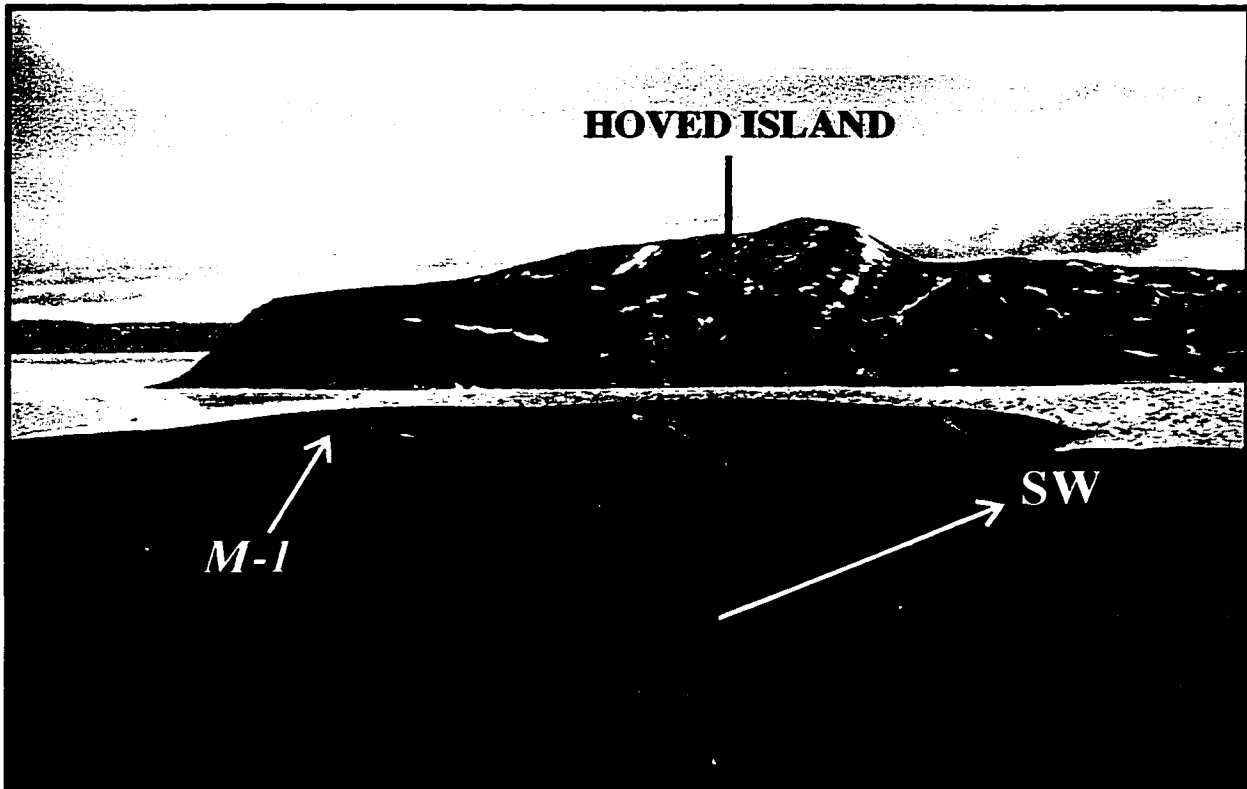


Figure 4.3. Morainal bank *M-1* looking south, showing gentle down-fiord slope

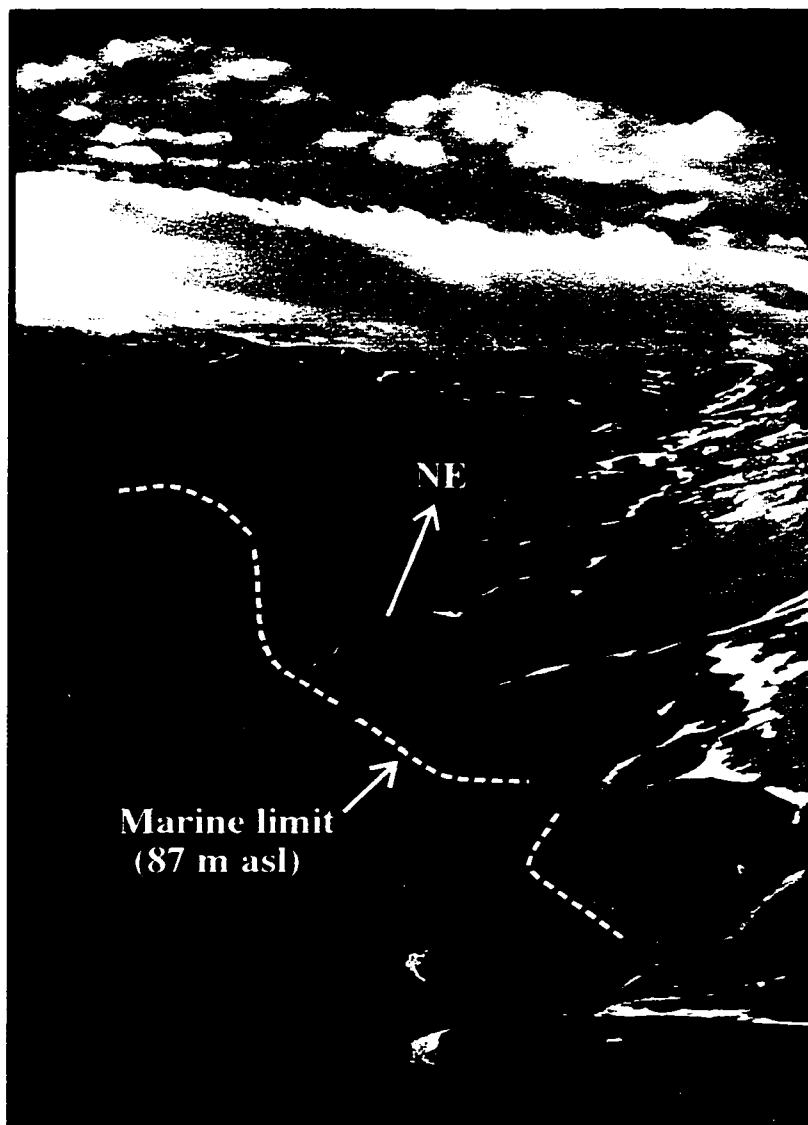


Figure 4.4. Washing limit on eastern Svendsen Peninsula interpreted as Holocene marine limit



8380 ± 100 BP (Beta 111705; Table 4.1; <sup>14</sup>C sample 4, Figure 4.1a). This provides a minimum age for the onset of ice-retreat into inner Baumann Fiord.

Twelve kilometers east of the 8.3 ka BP washing limit, northerly trending outcrops of sandy limestone are draped by marine sand and gravel. The upper limit of marine on-lap is recorded by a conspicuous break in slope, which is laterally continuous for 5 km (Figure 4.4). This is interpreted to mark Holocene marine limit, also at 87 m asl (Figure 4.1a).

#### 4.3.2 Southern Bjorne Peninsula

Marine limit along the coast of S Bjorne Peninsula is also indicated by an upper limit of marine on-lap, which descends from 108 m in the west of the field area, to 102 m asl adjacent to Gunnars Island, and 100 m asl at the mouth of Sor Fiord (Figure 4.1a).

A fifteen metre high section is exposed in the coastal lowlands of S Bjorne Peninsula (*S-1*; Figure 4.1a). Two units were recognized (Figure 4.5). The lower unit is ≤1 m thick, and comprised of a massive stony diamict with a coarse silt matrix. The diamict is dominated by rounded to sub-rounded carbonate pebbles and cobbles, although occasional rounded granite cobbles are also present. A distinct contact, with a seaward (northerly) dip of ≤5° separates the diamict from a ~14 m thick sequence of glaciomarine silt. In the lower 8 m of this sequence, the silt is massive to weakly stratified, whereas the upper part of the sequence consists of planar-bedded silt, which displays sharp contacts. The upper part of the sequence also contains occasional carbonate dropstones. No shells were recovered from either unit.

At the foot of the Schei Syncline, 15 km south of section *S-1*, an ice-contact delta is flanked by lateral meltwater channels draining uplands to the SE (*D-4*; Figures 4.1a and b). The delta marks marine limit at 85 m asl. Whole, paired valves of *H. arctica* recovered from foreset sand at 65 m asl dated 8050 ± 70 BP (Beta 111703; Table 4.1). Fluvial incision of fine-grained nearshore sediment distal to the delta slope (≤65 m asl) has exposed a 2 m high section (*S-2*; Figures 4.1a and 4.6). Two units were identified (Figure 4.7a and b). The lower unit is comprised of coarse silt (1.5 m thick) that displays fine ripple cross-laminations (Figure 4.8). This unit contains two lenticular gravel interbeds with erosional basal boundaries. The gravel interbeds range in thickness from 1-15 cm, are massive, matrix-supported and contain sub-rounded to sub-angular granule to cobble-sized carbonate clasts (Figure 4.9). This unit is conformably overlain

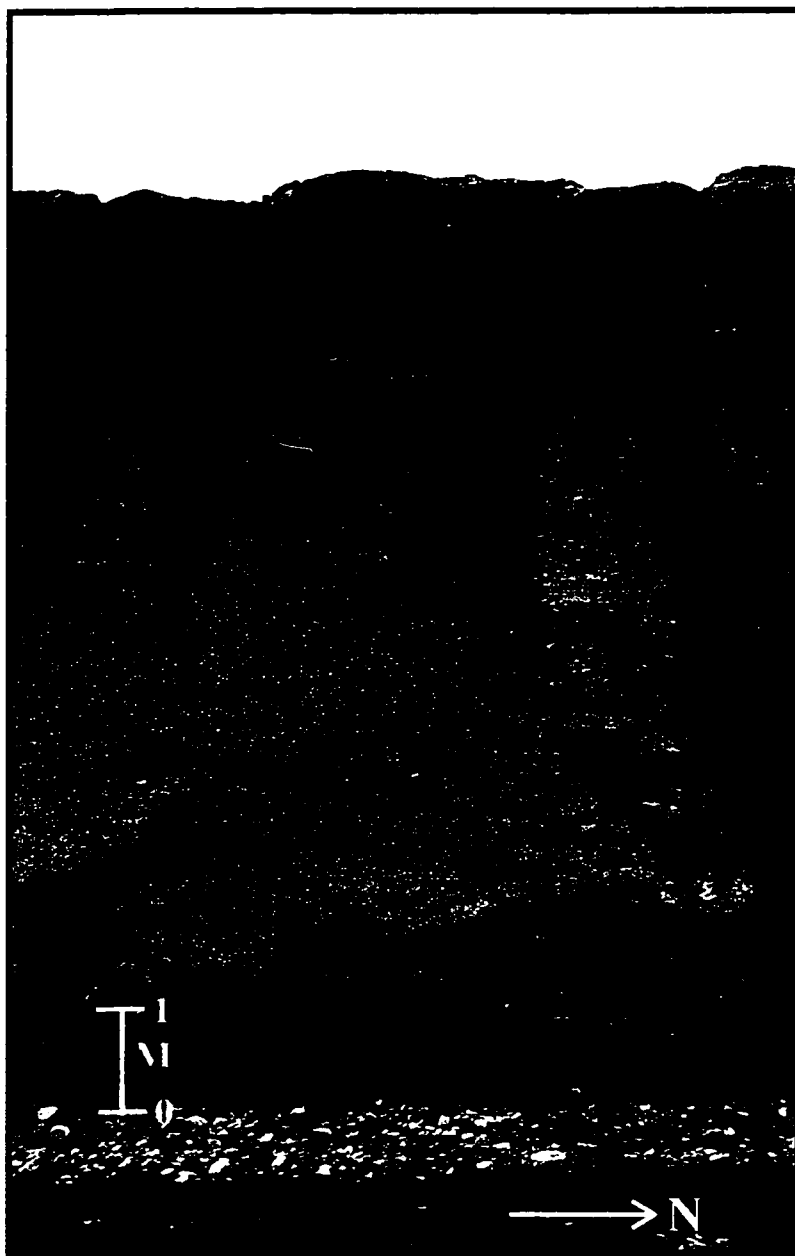


Figure 4.5. Photograph of section *S-1*, showing massive diamict overlain by crudely stratified to thinly laminated marine silt

by stratified diamict (50 cm thick), composed of scattered dropstones supported by a sandy silt matrix. Dropstones consist of sub-rounded to sub-angular carbonate pebbles and cobbles. Dropstone contacts are characterized by laminae exhibiting bending and penetrative deformation below the clast, and draped laminations above (cf., Thomas and Connell, 1985; Figure 4.10). Marine shells are absent within this sequence. A dated ice-contact delta at the head of Stenkul Fiord, 45 km east, indicates that Baumann Fiord was ice-free  $\geq 7.9$  ka BP (J. England, pers. comm., 1998).

## 4.4 Terrestrial Deglaciation

Former terrestrial ice margins are reconstructed principally by the distribution of lateral meltwater channels, which are presented in the following section.

### 4.4.1 *Eastern Svendsen Peninsula*

Three, low-gradient ( $\sim 11\%$ ), sub-parallel lateral meltwater channels have been eroded at successively lower elevations in the sidewall of the western highlands, close to the modern coastline (set D; Figure 4.1b). The upper channel ( $\sim 350$  m asl) extends for 2.5 km, and is eroded obliquely through NE-SW trending outcrops of sandy limestone. Two lower channels descend from  $\sim 220$  m asl to Holocene marine limit, where they terminate at deltas, 1.2 km to the south (Figures 4.1a and b). In the sidewall of the eastern highlands, low-gradient ( $7\%$ ) lateral meltwater channels descend from  $\sim 200$  m asl to Holocene marine limit (87 m asl) 1.6 km to the south (set E; Figures 4.1a and b).

On the lowlands of E Svendsen Peninsula ( $\leq 200$  m asl), two glacier lobes are defined by nested sets of lateral meltwater channels that flank the two main river valleys (Figure 4.1b). Towards the interior of E Svendsen Peninsula, adjacent drainage divides are flanked by lateral meltwater channels, nested along ice lobes retreating to the NE (sets F, G and H; Figure 4.1b).

### 4.4.2 *Southern Bjorne Peninsula*

Two lateral meltwater channels have been eroded on the eastern flank of the uplands in SE Bjorne Peninsula (set I; Figure 4.1b). The upper channel is incised at 270 m asl, and the lower channel (1.5 km long, 100 m wide) at 210 m asl. Five kilometers east, running parallel to the west coast of Sor Fiord, a straight, 30 m long ridge, with

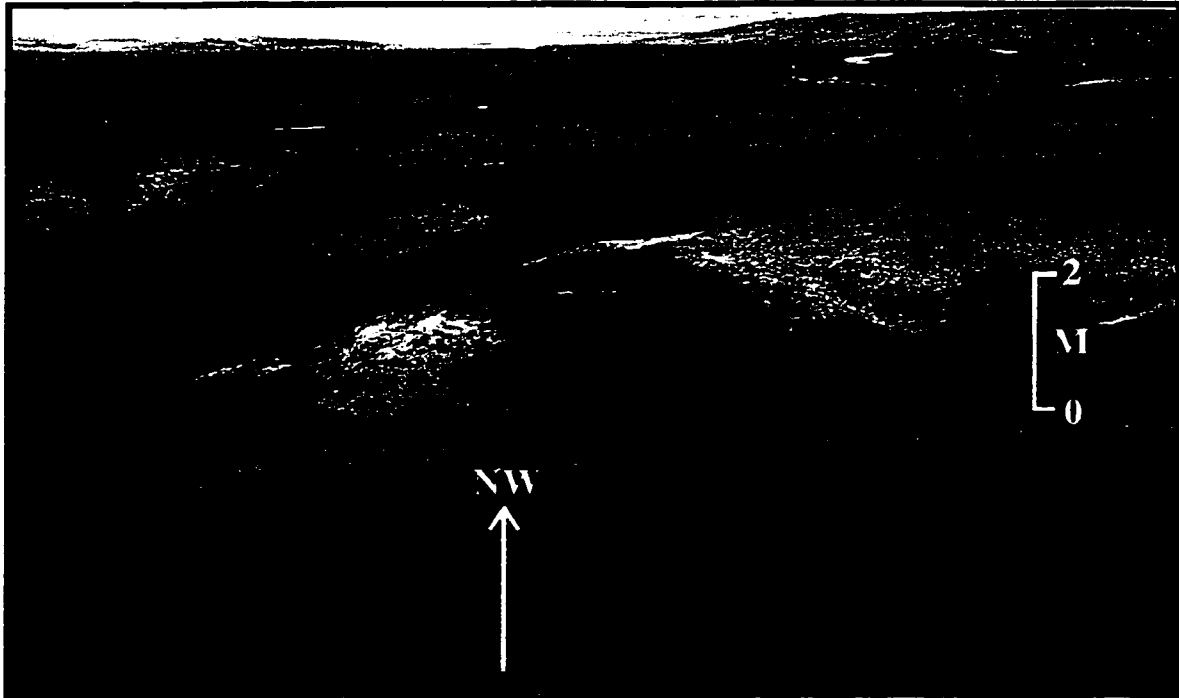


Figure 4.6. Fine-grained nearshore sediment distal to delta *D-4* . Vertical section at right (0-2 m) corresponds to section S-2 (Figure 4.7 a & b)

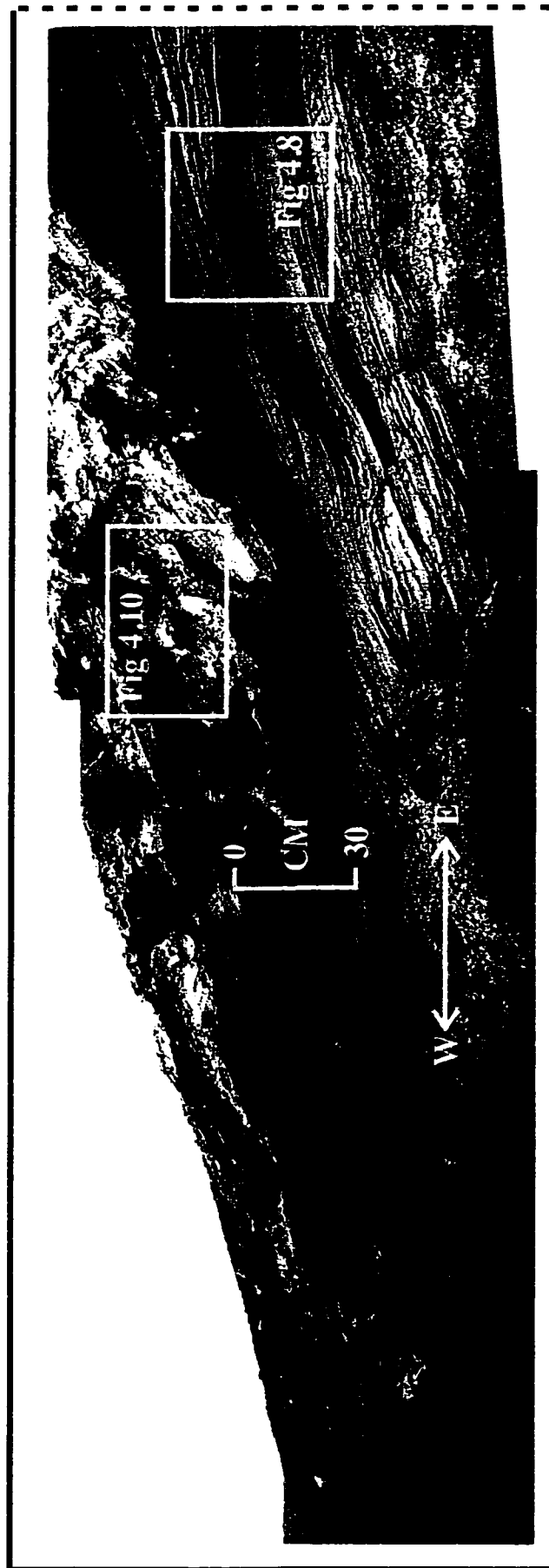


Figure 4.7a. Photograph of section S-2 (continued on figure 4.7b)

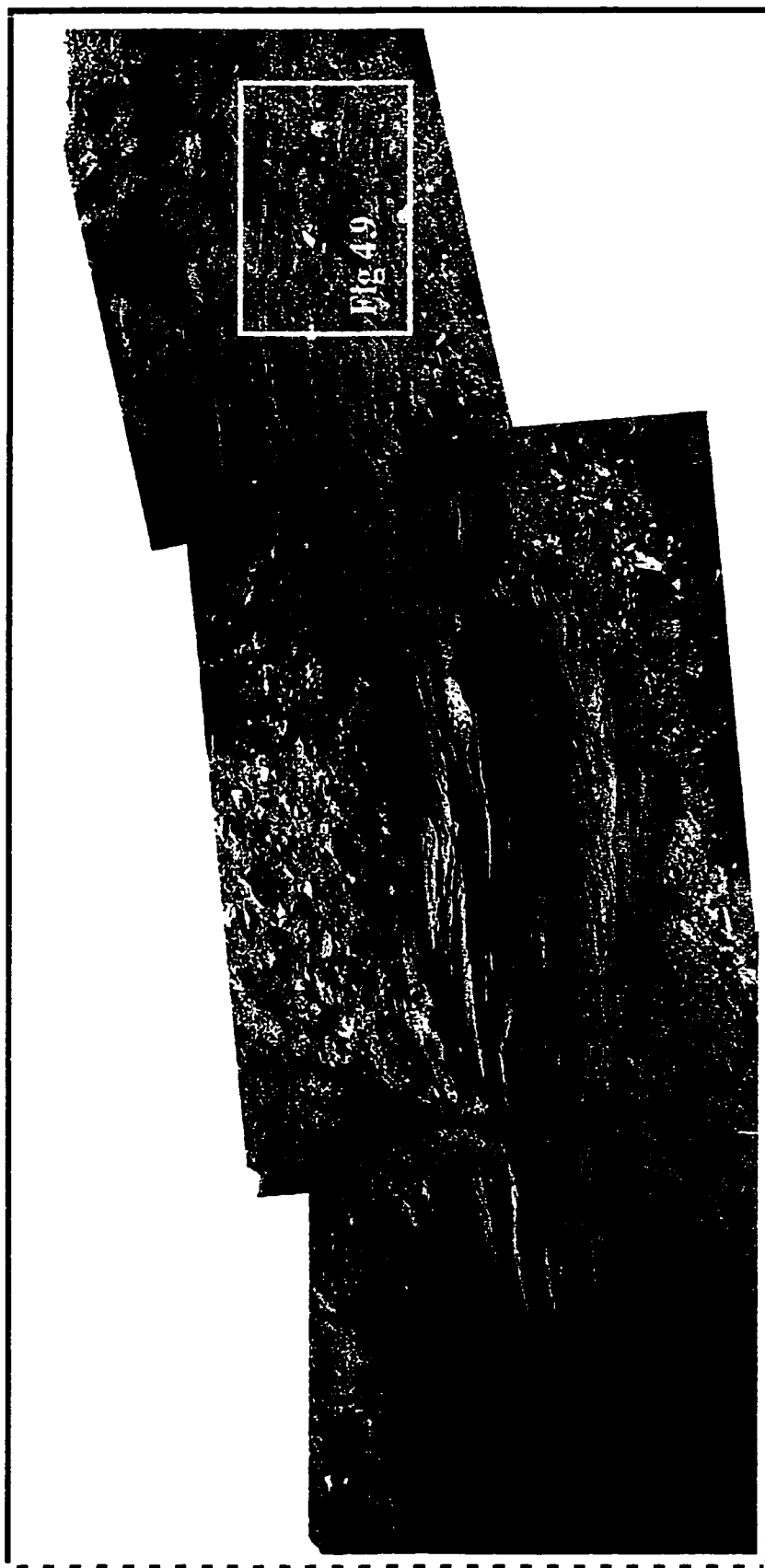


Figure 4.7b. Photograph of section S-2 (continued)

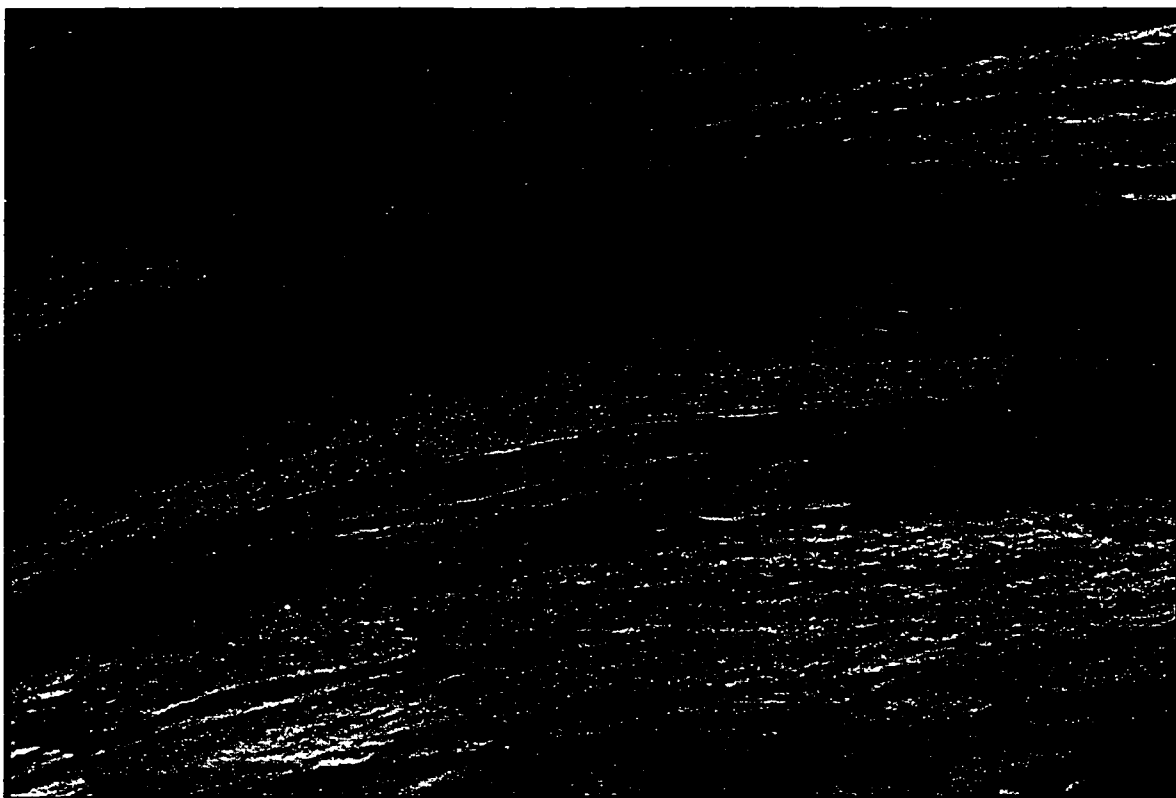


Figure 4.8. Lower unit of section S-2 (coarse silt) exhibiting bedding and cross-laminations



Figure 4.9. Gravel interbed within the lower unit of section *S*-2 (laminated coarse silt)



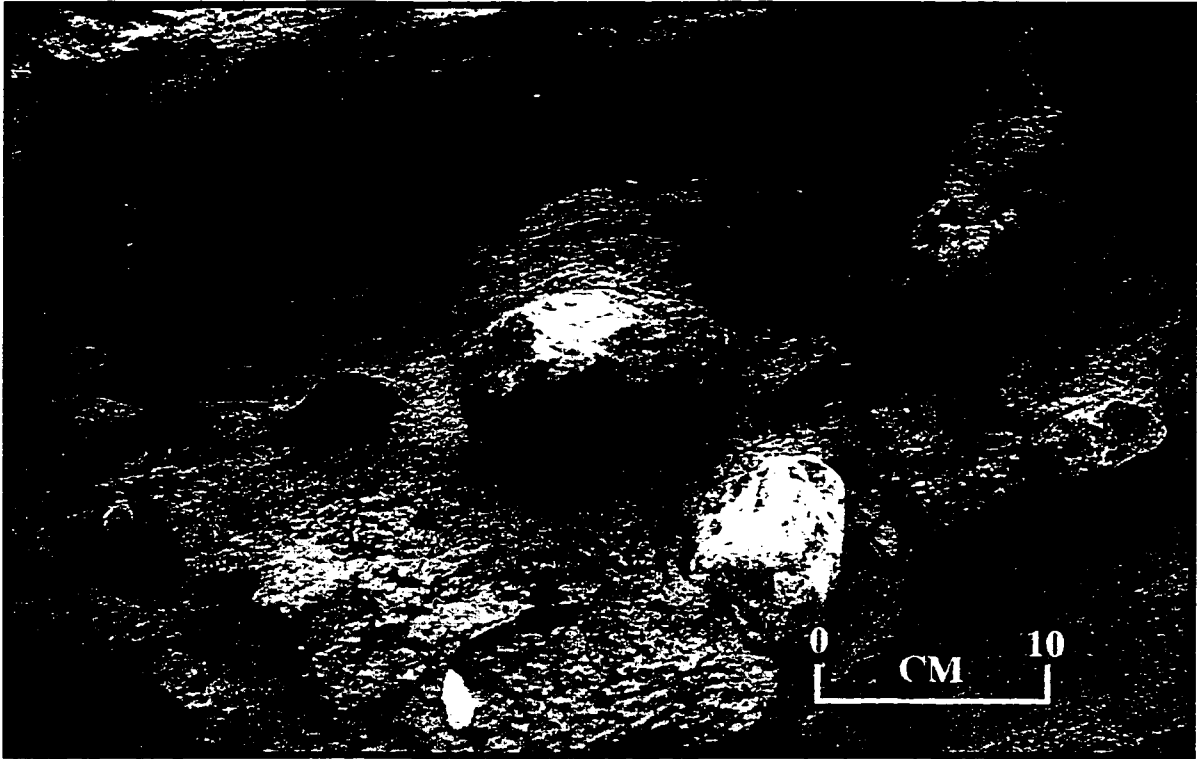


Figure 4.10. Dropstone contacts in section *S-2*, showing bending and penetrative deformation below the clasts and draped laminations above

steep east and west facing slopes occurs at 120 m asl (*M-2*; Figure 4.1b and 4.11). The ridge contains well rounded, moderately sorted limestone and granite cobbles and boulders, and based on its unstratified composition and morphology, is interpreted as a kame moraine, deposited by trunk ice occupying Sor Fiord.

Sub-parallel, low-gradient (12.5%) lateral meltwater channels incise rock/residuum and till blanket on the western flank of the SE Bjorne Peninsula uplands (set J; Figure 4.1b). These channels (~250 and 200 m asl) descend towards the modern coastline of central Baumann Fiord, 4 km to the north (Figure 4.1b).

Low elevation lateral meltwater channels ( $\leq 200$  m asl), nested towards the Schei Syncline, flank a large braided river in SE Bjorne Peninsula (Figure 4.1b). These lateral meltwater channels record ice retreat towards the Schei Syncline, and are responsible for deposition of delta *D-4*. Lateral meltwater channels nested towards the Schei Syncline also occur in south-central Bjorne Peninsula, where they are confined within the gentle slopes of a narrow braided river (Figure 4.1b).

A five kilometre long, E-W trending calcareous shale ridge (220 m high) outcrops in the central lowlands of Bjorne Peninsula (Figure 4.12). This ridge is incised by northward trending meltwater channels (Figure 4.1b). At the mouths of the two largest channels (~20 m wide), a 1.5 km<sup>2</sup> delta abuts the northern slope of the ridge (*D-5*; Figures 4.1a, b and 4.12). Fluvial incision during postglacial emergence has bisected the delta. The resultant surfaces on either side of the channel are both 140 m asl, and are characterized by an absence of marine shells. Extensive slumping along the outer edge of this delta presumably relates to failure along the boundaries of polygons, which are abundant on both surfaces.

## 4.5 Discussion

Lateral meltwater channels incised at successively lower elevations in the highlands of E Svendsen Peninsula and S Bjorne Peninsula record deglaciation along the terrestrial margins of tributary glaciers that became detached from the former trunk glacier that occupied Baumann Fiord. Evidence for trunk ice within central Baumann Fiord is recorded by striae and granite erratics on Hoved Island (Section 3.8) and ridge *M-1* (discussed below). The highest elevation lateral meltwater channels associated with dated glaciomarine sediments indicate that during the early Holocene, the tributary glaciers that occupied E Svendsen Peninsula and S Bjorne Peninsula were *at least* 350 m and 270 m thick, respectively.

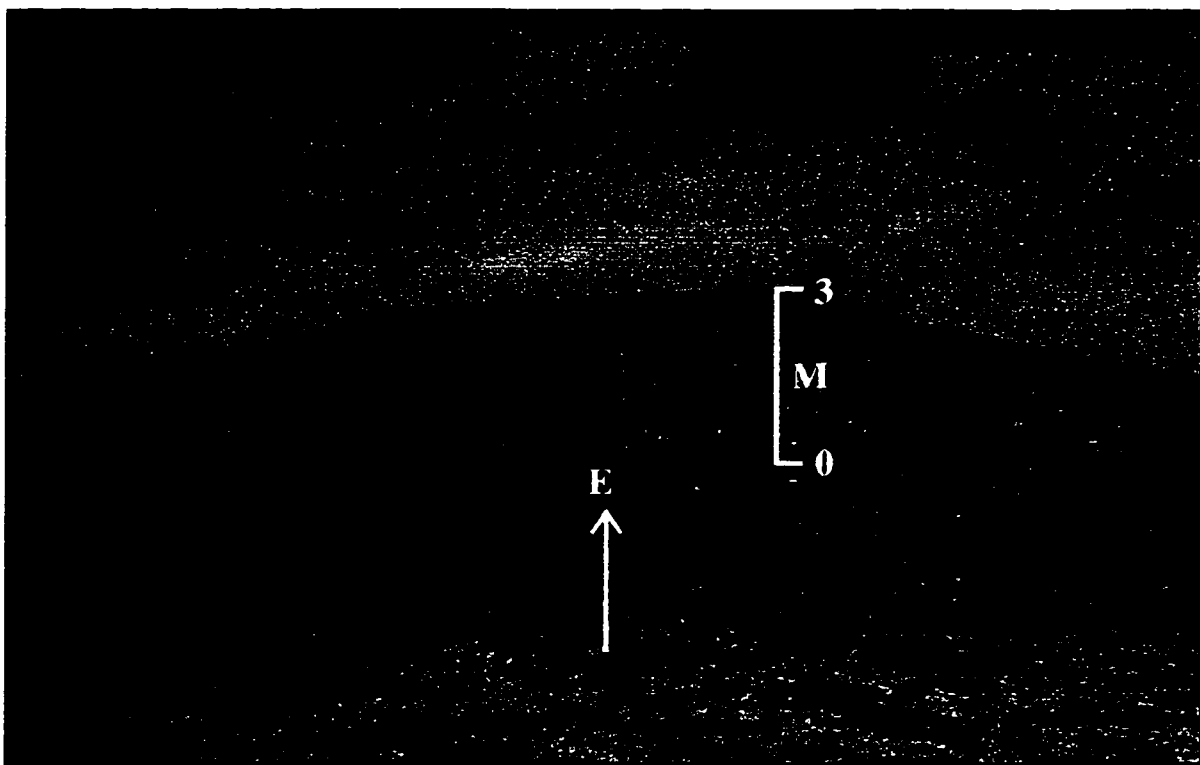


Figure 4.11. Kame moraine *M*-2, parallel to the axis of Sor Fiord

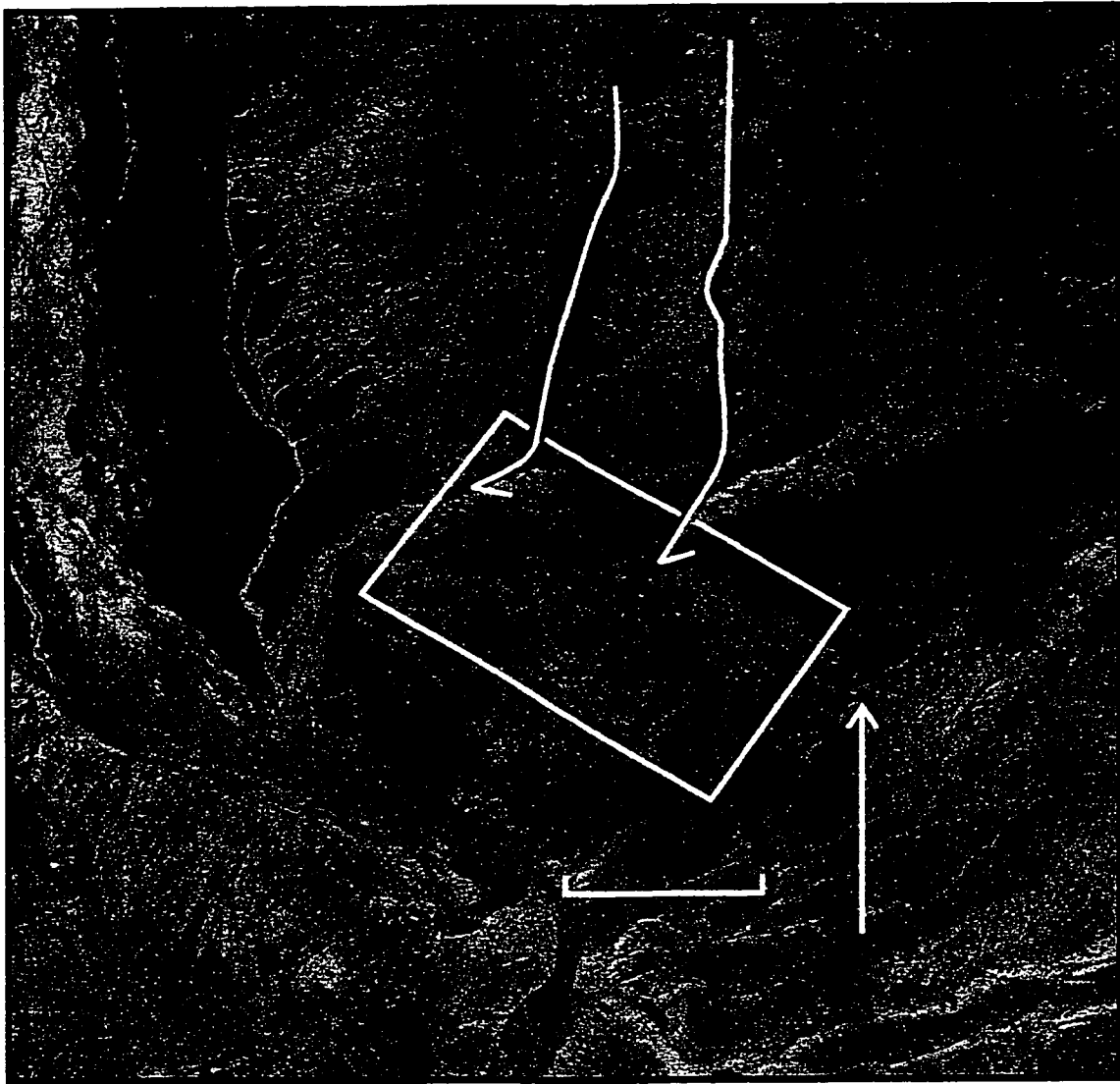


Figure 4.12. Air photo showing the relationship between the calcareous shale ridge and lateral meltwater channels on southern Bjorne Peninsula with delta *D-5*

Shells below delta *D-1* provide a *minimum* age of 8.1 ka BP for the initial re-entry of the sea, occasioned by ice-retreat from outer Baumann Fiord. Deglaciation at the head of Svarte Fiord is recorded by delta *D-3*, which contains shell fragments as old as 35.3 ka BP. These shells must have been recycled from an older deposit by the retreating glacier, which deposited delta *D-3* during Holocene deglaciation (cf., Dyke, in press a).

In Killam Lake, N Hoved Island, dated glaciomarine silt containing occasional dropstones records the re-entry of the sea into central Baumann Fiord at  $\geq 9.3$  ka BP (Smith, 1998). Additional sedimentary and radiocarbon data from Hoved Island record the progression of glaciomarine sedimentation from 8.6 ka BP to  $>8.0$  ka BP, in response to continued glacier retreat from Baumann Fiord. If delta *D-1* (107 m asl) is  $\geq 8.1$  ka BP, then marine limit on Hoved Island (102 m asl; England, pers. comm., 1998) ought to be of similar age, or younger. England (pers. comm., 1998) has recently obtained a date of 8.2 ka BP on a shell collected at 88 m asl on Hoved Island, suggesting that marine limit (14 m higher) is closer to 8.1 ka BP than it is to the 9.3 ka BP date in Killam Lake. Alternatively, the juxtaposition of younger shells (8.2 ka BP) close to marine limit with older dates (9.3 ka BP) may reflect slow initial emergence (cf. England, 1997). However, England (pers. comm., 1998) cautions the use of radiocarbon age determinations based on *P. arctica* samples, since this genus *may* provide older radiocarbon ages in relation to other mollusc species of a comparable age (c.f., Forman and Polyak, 1997).

A morainal bank (*M-1*) deposited by retreating trunk ice in Baumann Fiord occurs between E Svendsen Peninsula and Hoved Island (Figure 4.1b). This moraine coincides with a narrow (2 km) shallow ( $<100$  m) channel in Baumann Fiord which likely served as a pinning point during ice retreat (Figure 1.6). Eight kilometers up-fiord from Killam Lake, a washing limit is dated by shells  $\geq 8.3$  ka BP (8.9 ka cal years BP). Assuming that Hoved Island was deglaciated  $\sim 9.3$  ka BP (9.9 ka cal years BP) then during this 1000 year interval, the ice margin retreated into inner Baumann Fiord (to the site of the washing limit) at a rate of  $\sim 8$  m/yr. Slow retreat through central Baumann Fiord may have favoured grounding-line deposition, which would account for the formation of this morainal bank (cf., Powell, 1990, 1991). This likely corresponds to the location of a pinning point between E Svendsen Peninsula and S Hoved Island. However, Baumann Fiord was ice-free  $>7.9$  ka BP (8.3 ka cal years BP) indicating that continued retreat into the deeper basin of the inner fiord must have accelerated again,

reaching a rate of ~75 m/yr. These data suggest that Hoved Island slowed the rate of glacier retreat in central Baumann Fiord.

On S Bjorne Peninsula, the units described in section *S-1* are interpreted as deglacial sediments, associated with the retreat of ice from the south coast of central Baumann Fiord. Three alternatives for the genesis of the diamict are considered. Firstly, the diamict could be till, either deposited by a westward expansion of the Prince of Wales Icefield, or a northerly advance of the Sydkap Ice Cap. The abrupt contact represents erosion along the surface of the diamict associated with the marine transgression, recorded by the overlying silt. Secondly, the diamict could represent undermelt diamict, deposited by an ice shelf, or thirdly, it could represent subaquatic outwash, deposited by debris-flows from a retreating tidewater glacier (cf., Stewart, 1991). In all three cases, the diamict is considered to be associated with deglaciation, since the massive structure and abundance of pebbles and cobbles is suggestive of ice-proximal sedimentation. The fining-upward sequence of glaciomarine silt records the progressive settling of suspended sediment from turbid plumes (cf., Stewart, 1988, 1991). The transition from massive to thinly laminated silt may represent an increasingly distal position of the site in relation to the efflux. The presence of dropstones within the silt records rain-out of iceberg-rafted debris, combined with suspension settling of fines (Stewart, 1991; Ó Cofaigh, 1998a). This indicates that deglaciation of S Bjorne Peninsula involved the retreat of marine-based ice that had significant basal debris and a well-developed subglacial drainage system, and was therefore characterized by a warm-based thermal regime (cf., Ó Cofaigh, 1998a).

Sediments described in section *S-2* are also interpreted to be associated with the retreat of temperate marine-based ice across S Bjorne Peninsula. The ripple cross-laminated silts are interpreted as bottomset beds of the ice-contact delta, which were deposited by turbidity currents (Stewart, 1991). Gravel interbeds represent localized zones of scour and fill. Erosion is associated with strong efflux from the ice margin, or impingement of jet-flow on the underlying sediment (Powell, 1990). Deposition relates to a decrease in velocity from the efflux (Powell, 1990). Episodes of scour and fill are likely a function of fluctuations in jet-flow velocity caused by variations in subglacial meltwater discharge, episodic changes in the subglacial drainage system, or position of the site in relation to the efflux, possibly reflecting oscillations in the position of the ice margin (Powell, 1990; Ó Cofaigh, 1998a). The second unit (stratified diamict) relates to a different depositional regime. This unit could have been deposited by sediment remobilization, either caused by subaqueous slumping of the adjacent delta, or by

subaqueous debris flows from the glacier margin (cf., Stewart, 1991). However, neither the upper part of the silt sequence nor the basal part of the diamict displays evidence of erosion or shearing typically associated with slumping (cf., Benn and Evans, 1998). The nature of the bedding contacts that surround the isolated dropstones are consistent with rain-out, either from icebergs, or sedimentation from beneath a floating ice-margin (Gravenor *et al.*, 1984; Powell, 1984; Stewart, 1991). Consequently, the stratified diamict may represent dropstone diamict, deposited by icebergs during the final stages of marine-based deglaciation in southern Bjorne Peninsula, or undermelt diamict, deposited during a readvance of a floating ice-margin, which post-dated the deposition of *D-4*.

Following the retreat of temperate marine-based ice from central Baumann Fiord, encircling ice masses stabilized on E Svendsen Peninsula and S Bjorne Peninsula. Lateral meltwater channels (sets D and E) record drainage along the margins of a 25 km wide, 350 m thick cold-based glacier, enclosed within the highlands of E Svendsen Peninsula. Lateral meltwater channels also record continued ice-retreat across E Svendsen Peninsula, following the initial phase of downwasting. These channels suggest that recession involved thinning, concomitant with the NE retreat of two cold-based glacier lobes occupying the axes of adjacent river valleys. Towards the interior of E Svendsen Peninsula, lateral meltwater channels (sets F, G and H) indicate that subsequent recession was facilitated at the margins of smaller glacier lobes, which continued to retreat independently to the NE (Figure 4.1b).

On the uplands of SE Bjorne Peninsula, the distribution of lateral meltwater channels and a kame moraine (*M-2*) record the thinning and retreat of local ice (~270 m thick) towards the Sydkap Ice Cap. Towards the interior of the peninsula, lateral meltwater channels indicate that subsequent recession involved the progressive retreat of two glacier lobes through the Schei Syncline, towards the Sydkap Ice Cap (Figure 4.1b). The eastern lobe is defined by lateral meltwater channels flanking a large braided river in SE Bjorne Peninsula (Figure 4.1b). These channels record retreat of an  $\leq 18$  km wide glacier lobe occupying the axis of the river valley, and confirm that ice-marginal retreat was accompanied by marine transgression during the early Holocene. The second lobe is delineated by lateral meltwater channels confined within a narrow braided river valley in south-central Bjorne Peninsula (Figure 4.1b). These document the southward retreat of a  $\leq 6$  km wide glacier lobe.

Based on the association of delta *D-5* with lateral meltwater channels on the left flank of the eastern glacier lobe, two alternatives for its genesis are considered. Firstly,

the delta could have prograded from the mouth of the lateral meltwater channel into a marine embayment on S. Bjorne Peninsula. However, the elevation of the delta (140 m asl) is above Holocene marine limit recorded elsewhere in the field area (108 to 85 m asl), and no shells were observed on its surfaces. Alternatively, the delta could have been deposited in a proglacial lake, either accumulating between the margins of the Sydkap Ice Cap during its retreat around the calcareous shale ridge, or between retreating local ice lobes and trunk ice in Baumann Fiord.

## 4.7 Summary

Geomorphic and sedimentary signatures record the Holocene deglacial history of central Baumann Fiord. Lateral meltwater channels eroded at successively lower elevations in the highlands of E Svenden Peninsula and S Bjorne Peninsula record retreat along the terrestrial margins of tributary glaciers which sustained trunk ice within central Baumann Fiord. The distribution of radiocarbon-dated glaciomarine sediments record the sequential entry of marine fauna into Baumann Fiord, concomitant with the retreat of the warm-based trunk glacier. These data provide a minimum estimate on the chronology of ice-retreat along Baumann Fiord.

Deglaciation of N. Hoved Island occurred  $\geq 9.3$  ka BP (Smith, 1998). Slow retreat between  $\geq 9.3$  and  $\sim 8.3$  ka BP favoured the deposition of a morainal bank at a grounding-line that was pinned between E Svendsen Peninsula and S Hoved Island. Continued glacier retreat into the deeper basin of inner Baumann Fiord proceeded more rapidly, culminating with the removal of ice from Baumann Fiord  $\geq 7.9$  ka BP.

Ice-contact sediments deposited at Holocene marine limit indicate that as glacier retreat proceeded onshore, ice masses encircling central Baumann Fiord stabilized on E Svendsen Peninsula and S Bjorne Peninsula. Slower rates of land-based retreat may account for the distribution of more widespread glaciogenic landforms, which document the retreat of topographically-constrained, cold-based glacier lobes towards the Prince of Wales Icefield and Sydkap Ice Cap. This reconstruction supports the two-step model of ice retreat for W and E Ellesmere Island (cf., Model A, Hodgson, 1985; Ó Cofaigh, 1998a; England, 1998a, in press). Hodgson (1985) suggested that conspicuous glaciogenic landforms contacting Holocene glaciomarine sediments at the heads of many fiords in west-central Ellesmere Island could record ice-marginal stillstand following the retreat of a regional ice sheet, possibly in response to climatic cooling.



## CHAPTER FIVE

### 5.1 Last Glacial Maximum

On E Svendsen Peninsula, granite dispersal trains and striated bedrock record the SW advance of regional (granite-carrying) ice from a divide over an expanded Prince of Wales Icefield during the LGM. Southwesterly flowing ice sustained a trunk glacier in central Baumann Fiord, which overrode Hoved Island. During early Holocene deglaciation, ice on E Svendsen Peninsula was  $\geq 350$  m thick. Based on a mean water depth of 300 m (Canadian Hydrographic Service, 1985; Figure 1.6) these data suggest that central Baumann Fiord was occupied by a trunk glacier  $\geq 650$  m thick. Although erratics and striae that indicate E Svendsen Peninsula has been overridden by ice  $\geq 615$  m thick are of an unknown age, Chlorine-36 dates on granite erratics at similar elevations on Raanes Peninsula (Figure 1.2) indicate that dispersal trains may have been active during the late Wisconsinan (Ó Cofaigh, 1998c). Consequently, trunk ice in central Baumann Fiord *may* have been  $\geq 915$  m thick during the LGM. Moreover, the distribution of granite erratics across Bjorne Peninsula suggest that regional ice coalesced with the Sydkap Ice Cap and flowed west towards Norwegian Bay. During the early Holocene, ice  $\geq 270$  m thick retreated across southern Bjorne Peninsula towards the Sydkap Ice Cap. However, granite erratics of unknown age indicate that the Schei Syncline has been covered by regional ice  $\geq 700$  m thick.

England (1998a) proposed that ice-flow from the Prince of Wales Icefield towards Eureka Sound was enhanced by the confluence of E Ellesmere ice with Greenland ice in Nares Strait during the LGM. To the east of the field area, near glacier 7A-45 (Figure 1.3), radiocarbon-dated sedge rhizomes from a bed of organic debris directly underlying till indicate that such an advance *may* have occurred  $\leq 19.7$  ka BP (Blake, 1992).

The Prince of Wales Icefield displays longitudinal asymmetry, with the ice on the east side being significantly thicker than that on the west (Koerner, 1979). The surface elevation of the Prince of Wales Icefield displays latitudinal asymmetry, decreasing from 2350 m, west of Jokel Fiord, to 1288 m, south of Makinson Inlet (Canadian Topographic Survey, 1975; Blake, 1992; Figures 1.2 and 5.1). Such asymmetry relates to topoclimatic influences (cf., Miller *et al.*, 1975; Koerner, 1979; Section 1.7). It is proposed that this ice surface gradient was accentuated during the last

glaciation. This is because the magnitude of outflow on the eastern side of the Ellesmere Island ice divide would presumably have increased to the south, due to the diminished effect of buttressing in S Nares Strait (south of Smith Sound), where drawdown would have been promoted by enhanced calving in N Baffin Bay (cf., Blake, 1992). The magnitude of outflow from the western side of the Ellesmere Island ice divide likely reflected this gradient, also decreasing to the south. This interpretation explains why the glacial geologic evidence indicates that Baumann Fiord was a significant outlet for ice-flow draining the NE sector of Prince of Wales Icefield during the LGM. These data suggest that the southern limit of westward flow from the Prince of Wales Icefield was in the vicinity of the Schei Syncline, and support the proposal of Ó Cofaigh (1998c) that a granite dispersal train from Svendsen Peninsula was deflected into Baumann Fiord, which coalesced with southerly-flowing trunk ice exiting Eureka Sound, and flowed into Norwegian Bay. This may have extended through Norwegian Bay, and onto the western Arctic Islands (England, 1998b)

Geomorphic and sedimentary signatures indicate that the initial stages of early Holocene deglaciation in central Baumann Fiord were characterized by ice retreat along the terrestrial margins of tributary glaciers occupying Svendsen and Bjorne peninsulas, concomitant with the retreat of a marine-based trunk glacier characterized by a warm-based thermal regime (Section 4.5). This interpretation is consistent with studies conducted elsewhere in the high Arctic (cf., Stewart, 1988; Evans, 1988; Ó Cofaigh, 1998a and c). Deglaciation likely relates to a combination of internal (changes in mass balance and basal ice conditions, in response to early Holocene warming) and external (eustatic sea level rise) forcing mechanisms. Powell (1991) remarked that climate (through its influence on glacier mass balance and ice temperature) was the first order control governing the fluctuations of tidewater glacier termini. Koerner and Fisher (1990) reported that the melt record of the Agassiz Ice Cap revealed highly negative mass balance during the early to mid-Holocene, which resulted in the retreat of high Arctic glaciers at, or before 9-10 ka BP. Bradley (1990) presented considerable evidence in support of a mid-Holocene warm period, and remarked that these data reflected *continued* warm conditions from the early Holocene, when summer temperatures may have been even higher. Van der Veen (1996) illustrated that the basal conditions of tidewater glaciers (e.g., basal ice temperature and subglacial hydrology) strongly influenced their rate of thinning, which in turn determined their rate of calving. Moreover, England (1992, in press) and Ó Cofaigh (1998a) proposed that rapid disintegration of Innuitian ice within the marine channels of the QEI may have been

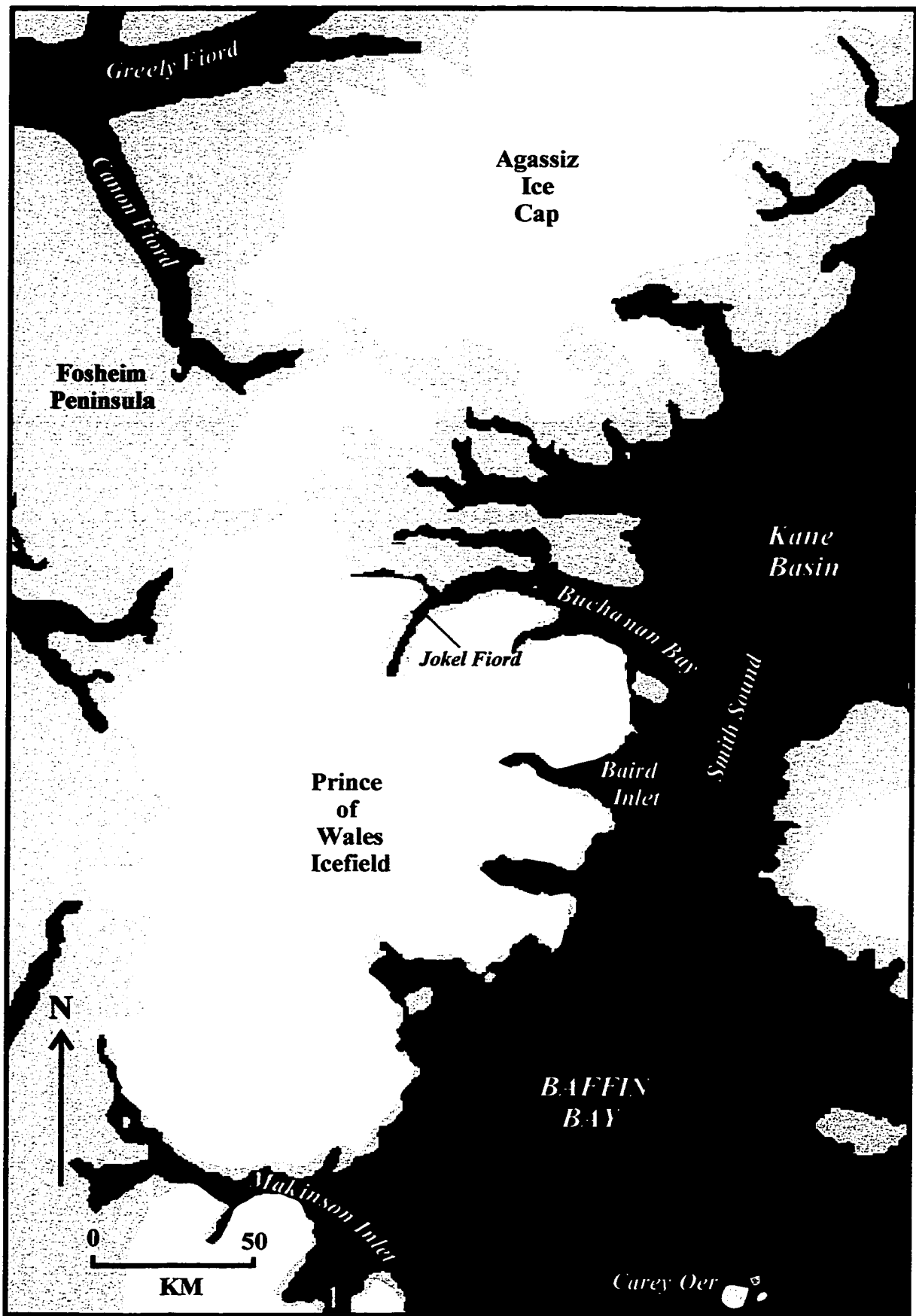


Figure 5.1. Eastern Ellesmere Island, showing position of contemporary ice caps (shaded)

initiated or enhanced by calving, in response to eustatic sea level rise >9.2 ka BP (cf., Fairbanks 1989; Tushingham and Peltier, 1991). However, the relative influence of these factors on the Late Quaternary deglacial history of SW Ellesmere Island remains to be determined. Marine-based ice retreat in Baumann Fiord was punctuated by an interval of stabilization on Hoved Island. Following the removal of marine-ice from Baumann Fiord, stabilization of encircling ice masses on Svendsen Peninsula and Bjorne Peninsula facilitated slower rates of land-based retreat towards the Prince of Wales Icefield and Sydkap Ice Cap, respectively.

## 5.2 Relative Sea Level History

Holocene marine limit recorded in central Baumann Fiord is 107 m asl (8.5 ka BP; Site 1, Table 4.1). Accounting for the eustatic fall in sea level at 8.5 ka BP (~30 m; England, 1992) these data indicate the crustal depression associated with the glaciation of central Baumann Fiord was  $\geq 137$  m. According to the principle of glacioisostasy (crustal depression beneath an ice mass is 0.3 times ice thickness; cf., Andrews, 1970) these data provide a *minimum* estimate of 411 m for ice thickness in central Baumann Fiord during the last glaciation.

Marine limit in central Baumann Fiord descends from 107 m asl at the mouth of Svarte Fiord ( $\geq 8.1$  ka BP; Site 2, Figure 4.1a and Table 4.1), to 102 m asl on Hoved Island ( $\geq 8.2$  ka BP; Site 1, Figure 4.1a) to 87 m asl on E Svendsen Peninsula ( $\geq 8.3$  ka BP; Site 4, Figure 4.1a). Postglacial isobases drawn on the 8.0 ka shoreline exhibit a rise to the NW, out of the fiord, towards Eureka Sound (Figure 5.2). These data are consistent with the isobases drawn on the 8.5 ka BP shoreline by Ó Cofaigh (1998c) which also show a westward rise towards Eureka Sound. England and Ó Cofaigh (1998) attributed a closed cell of highest emergence (150 m asl) along Eureka Sound to an axis of greatest glacioisostatic unloading, where the Innuitian Ice Sheet was formerly thickest.

## 5.3 Future Research

Outflow from the Ellesmere ice divide was facilitated by trunk glaciers centred through Bay Fiord and southern Eureka Sound (Ó Cofaigh, 1997, 1998b and c), and Baumann Fiord. These ice masses converged towards Norwegian Bay where they likely

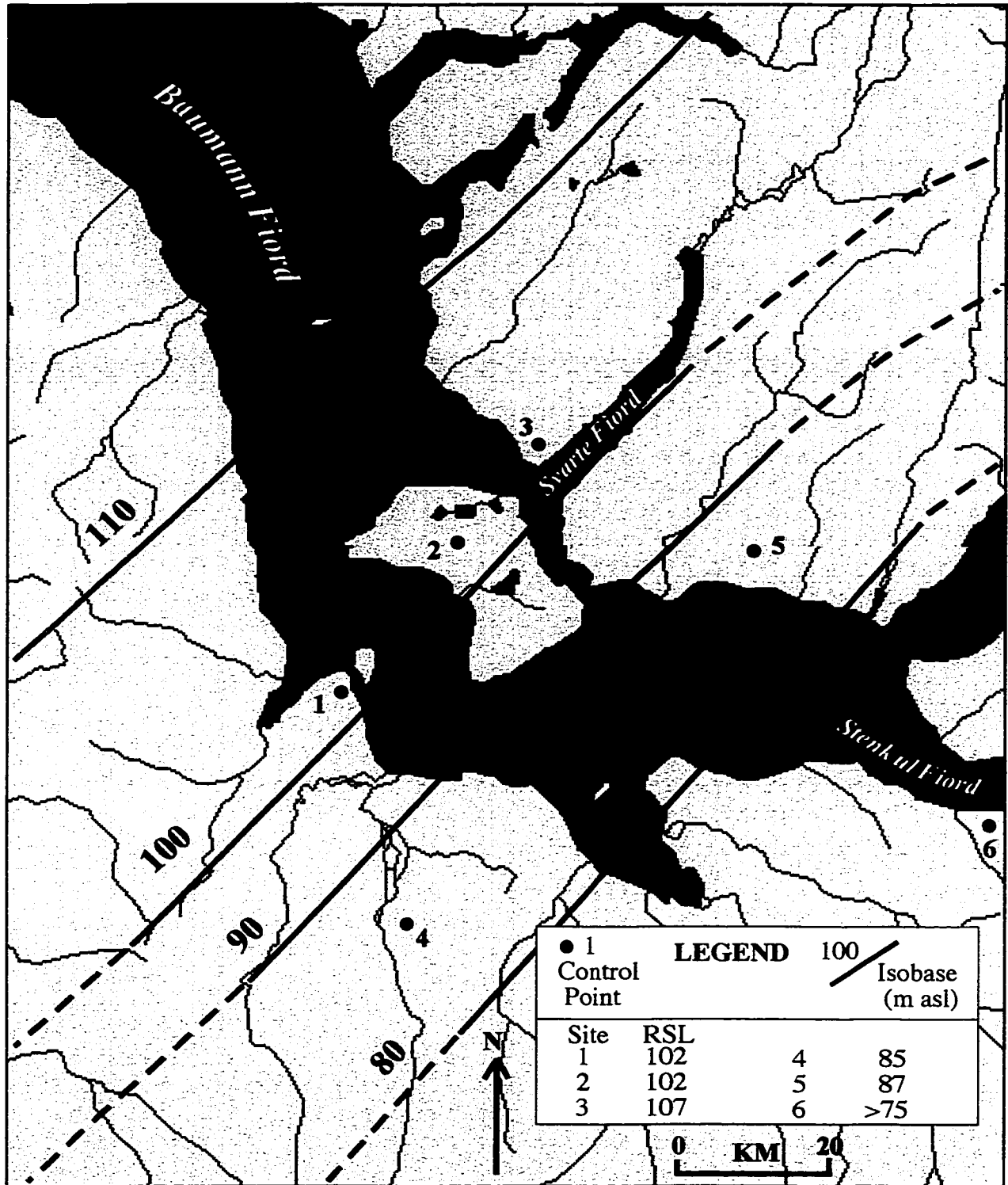


Figure 5.1. Postglacial isobases (provisional) drawn on the 8.0 ka BP shoreline in central Baumann Fiord. This reconstruction utilizes an 8.5 ka BP shoreline (shown in red) constructed by O' Cofaigh (1998c)

flowed west to the undefined limit of the Innuitian Ice Sheet in the western Arctic Islands (Hodgson, 1989). Moreover, outflow on the opposite (NW) side of the NE-SW trending ice divide extending across the central QEI (Dyke, in press b) would have constituted an additional ice source filling Norwegian Bay (England, 1998b). Therefore, Norwegian Bay was likely an important outlet on the west side of the Innuitian Ice Sheet. Evacuation of ice to the NW would have been facilitated by Massey Sound (200 km long, 40 km wide) that separates Amund Ringnes Island from Axel Heiberg Island (England, 1998b; Figure 1.1). To date, there have been only reconnaissance surveys conducted on the north-central QEI (Sverdrup and adjacent islands; Hodgson, 1982).

This uninvestigated western sector of the QEI constitutes the next phase of field research. Important issues to be addressed include: (1) determining the extent, origin and configuration of Innuitian ice penetration into and through Norwegian Bay, and its interaction with alpine glaciers on S Axel Heiberg Island and additional Innuitian Ice to the south (Dyke, in press b), (2) determining the origin of granite erratics reported in the western QEI (Hodgson, 1982) and if glacial, establishing whether they were transported by northward flowing Laurentide ice, or westward flowing Innuitian ice, or whether any of these erratics have a different origin (i.e., Tertiary fluvial erratics), (3) establishing whether granite erratic dispersal relates to a hypothesized ice stream centred through Massey Sound (England, 1998b), (4) documenting the chronology and style of ice retreat. Furthermore, because a close association may have existed between the deglacial history of the Innuitian Ice Sheet and the marine channels of the QEI, relating the history of its retreat to clastic sedimentary records from the adjacent Arctic Ocean Basin (cf., Bischof and Darby, 1997) may provide a stimulating opportunity for future research.

## CHAPTER SIX

Alt, B.T. and Maxwell, J.B. (1990) The Queen Elizabeth Islands: A case study for arctic climate data availability and regional climate analysis. In *Symposium on the Canadian Arctic Islands, Canada's missing dimension*. Harrington, C.R. (ed) National Museum of Natural Sciences, Ottawa.

Andrews, J.T. (1970) A geomorphic study of postglacial uplift with particular reference to Arctic Canada. Institute of British Geographers, Special Publication 2, London, 156p.

Bednarski, J. (1995) Glacial advances and stratigraphy in Otto Fiord and adjacent areas, Ellesmere Island, Arctic Canada. *Canadian Journal of Earth Sciences* **32**: 52-64.

Bednarski, J. (1998) Quaternary history of Axel Heiberg Island, bordering Nansen Sound, northwest Territories, emphasizing the last glacial maximum. *Canadian Journal of Earth Sciences* **53** No 5: 520-533.

Bell, T. (1992) Glacial and sea level history of western Fosheim Peninsula, Ellesmere Island, Arctic Canada. Unpublished Ph.D. thesis, University of Alberta, Edmonton, Alberta.

Bell, T. (1996) The last glaciation and sea level history of Fosheim Peninsula, Ellesmere Island, Canadian High Arctic. *Canadian Journal of Earth Sciences* **33**: 1075-1086.

Benn, D.I. and Evans, D.J.A. (1998) *Glaciers and Glaciation*. Arnold, London.

Bischof, J.F. and Darby, D.A. (1997) Mid-to late Pleistocene ice drift in the west Arctic Ocean: Evidence for a different circulation in the past. *Nature* **277**: 74-78.

Blake, W. Jr. (1970) Studies of glacial history in Arctic Canada. *Canadian Journal of Earth Sciences* **7**: 634-664.

Blake, W. Jr. (1972) Climatic implications of radiocarbon-dated driftwood in the Queen Elizabeth Islands, Arctic Canada. In *Climatic change in the arctic areas during the last ten thousand years*. Vasari, Y., Hyvarinen, H. and Hicks, S. (eds).

Blake, W. Jr. (1975) Radiocarbon age determination and postglacial emergence at Cape Storm, southern Ellesmere Island. *Geografiska Annaler* **57A**: 1-71.

Blake, W. Jr. (1977) Glacial sculpture along the east-central coast of Ellesmere Island, Arctic Archipelago. In Report of activities, part C. *Geological Survey of Canada*, Paper 77-1C, pp. 107-115.

Blake, W. Jr. (1992) Holocene emergence at Cape Herschel, east-central Ellesmere Island, Arctic Canada: implications for ice sheet configuration. *Canadian Journal of Earth Sciences* **29**: 1958-1980.

Blake, W. Jr., Jackson, H.R. and Currie, C.G. (1996) Seafloor evidence for glaciation, northernmost Baffin Bay. *Bulletin of the Geological Society of Denmark* **23**: 157-168.

Bradley, R.S. (1990) Holocene paleoclimatology of the Queen Elizabeth Islands, Canadian High Arctic. *Quaternary Science Reviews* **9**: 365-384.

Canadian Hydrographic Service (1985) Chart 7950, Jones Sound, Norwegian Bay and Queens Channel (1: 500 000). Department of the Environment, Ottawa.

Canadian Topographic Survey (1975) Landsat-1 Multispectral Image (1: 1 000 000). Department of Energy, Mines and Resources, Ottawa.

Dyke, A.S. (1983) Quaternary Geology of Somerset Island, District of Franklin. *Geological Survey of Canada*, Memoir 404.



- Dyke, A. S. (1993) Landscapes of cold-centred late Wisconsinan ice caps, Arctic Canada. *Progress in Physical Geography* **7** 1 (2): 223-247.
- Dyke, A.S. (in press a) Last glacial maximum and deglaciation of Devon Island, Arctic Canada: Support for an Innuitian Ice Sheet. *Quaternary Science Reviews*
- Dyke, A.S. (in press b) Holocene deleveilling of Devon Island, Arctic Canada: Implications for ice sheet geometry. *Canadian Journal of Earth Sciences*
- Dyke, A.S. and Prest, V.K. (1987) Late Wisconsinan and Holocene history of the Laurentide Ice Sheet. *Géographie physique et Quaternaire* **41**: 237-263.
- England, J. (1976a) Late Quaternary glaciation of the Queen Elizabeth Islands, Northwest Territories, Canada: alternative models. *Quaternary Research* **6**: 185-202.
- England, J. (1976b) Postglacial isobases and uplift curves from the Canadian and Greenland High Arctic. *Arctic and Alpine Research* **8**: 61-78.
- England, J. (1983) Isostatic adjustments in a full glacial sea. *Canadian Journal of Earth Sciences* **20**: 895-917.
- England, J. (1986) A paleoglaciation level for north-central Ellesmere Island, NWT, Canada. *Arctic and Alpine Research* **18**: 217-222.
- England, J. (1987) Glaciation and the evolution of the Canadian high arctic landscape. *Geology* **15**: 419-424.
- England, J. (1990) The late Quaternary history of Greely Fiord and its tributaries, west-central Ellesmere Island. *Canadian Journal of Earth Sciences* **27**: 255-270.
- England, J. (1992) Postglacial emergence in the Canadian High Arctic: integrating glacioisostasy, eustasy, and late deglaciation. *Canadian Journal of Earth Sciences* **29**: 984-999.

England, J. (1997) Unusual rates and patterns of Holocene emergence, Ellesmere Island, Arctic Canada. *Journal of the Geological Society, London* **154**: 781-792.

England, J. (1998a) Support for the Innuitian Ice Sheet in the Canadian High Arctic during the Last Glacial Maximum. *Journal of Quaternary Science* **13**: 275-280.

England, J. (1998b) Consensus on the Innuitian Ice Sheet during the last glacial maximum: new evidence and opportunity. *GSA Abstracts with programs*, vol **30**, no. 7.

England, J. (in press) Coalescent Greenland and Innuitian ice during the last glacial maximum: revising the Quaternary of the Canadian High Arctic. *Quaternary Science Reviews*.

England, J., Sharp, M., Lemmen, D.S. and Bednarski, J. (1991) On the extent and thickness of the Innuitian Ice Sheet: postglacial-adjustment approach: Discussion. *Canadian Journal of earth Sciences* **28**: 1689-1695.

England, J. and Ó Cofaigh, C. (1998) Deglacial sea level along Eureka Sound: The effects of ice retreat from a central basin to alpine margins (Abstract). *Joint Meeting of the Geological Association of Canada, Quebec, Canada* **16**: A-52.

Evans, D.J.A. (1988) Glacial geomorphology and Late Quaternary history of Phillips Inlet and the Wootton Peninsula, Northwest Ellesmere Island, Canada. Unpublished Ph.D. thesis, University of Alberta, Edmonton, Alberta.

Fairbanks, R.G. (1989) A 17,000 year glacio-eustatic sea level record: influence of glacial melting rate on the Younger Dryas event and deep ocean circulation. *Nature* **342**: 637-642.

Fisheries and Environment, Canada (1978) An Arctic Atlas: Arctic Marine Oilspill Program Report. Environmental Protection Service, Ottawa, Ontario.

- Forman, S.L. and Polyak, L. (1997) Radiocarbon content of pre-bomb marine mollusks and variations in the  $^{14}\text{C}$  reservoir age for coastal areas of the Barents and Kara seas, Russia. *Geophysical Research Letters* **24**: 885-888.
- Frisch, T. (1988) Reconnaissance geology of the Precambrian shield of Ellesmere, Devon and Coburg islands, Canadian Arctic archipelago. *Geological Survey of Canada, Memoir* 409.
- Funder, S. and Hansen, L. (1996) The Greenland ice sheet- a model for its culmination and decay during and after the last glacial maximum. *Geological Society of Denmark Bulletin* **42**: 137-152.
- Geological Survey of Canada (1970) Economic Geology Report No. 1. Maps and Charts (5th edition). Department of Energy, Mines and Resources, Ottawa, Canada.
- Gravenor, C.P., von Brunn, V. and Dreimanis, A. (1984) Nature and classification of waterlain glaciogenic sediments, exemplified by Pleistocene, Late Palaeozoic and Late Precambrian deposits. *Earth Science Reviews* **20**: 105-166.
- Hättestrand, C. and Stroeve, A.P. (1996) Field evidence for Wet-Based Ice Sheet Erosion from the south-central Queen Elizabeth Islands, Northwest Territories, Canada. *Arctic and Alpine Research* **28** (4): 466-474.
- Hodgson, D.A. (1982) Surficial materials and geomorphological processes, western Sverdrup and adjacent islands, District of Franklin. *Geological survey of Canada, Paper* 81-9.
- Hodgson, D.A. (1985) The last glaciation of west-central Ellesmere Island, Arctic Archipelago, Canada. *Canadian Journal of Earth Sciences* **22**: 347-368.
- Hodgson, D.A. (1989) Quaternary stratigraphy and chronology (Queen Elizabeth Islands). In *Quaternary Geology of Canada and Greenland*, Fulton, R.J. (ed); Geological Survey of Canada, Geology of Canada, No.1, pp. 452-459.

- Kerr, J.W. (1981) Evolution of the Canadian Arctic Islands: transition between the Atlantic and Arctic Oceans. In *The Ocean Basin Margin, Volume 5, The Arctic Ocean*. Nairn, A.E.M., Churkin, M. Jr., Stehli, F.G. (eds) Plenum Press, New York, 115-199.
- Koerner, R.M. (1979) Accumulation, ablation, and oxygen isotope variations on the Queen Elizabeth Islands ice caps, Canada. *Journal of Glaciology* **22**: 25-29.
- Koerner, R.M., and Fisher, D.A. (1990) A record of Holocene summer climate from a Canadian high-Arctic ice core. *Nature* (London) **343**: 630-631.
- Maxwell, J.B. (1981) Climatic regions of the Canadian Arctic Islands. *Arctic* **34**: 224-240.
- Mayr, U. (1973) Lithologies and depositional environments of the Allen Bay-Read Bay Formations (Ordovician-Silurian) on Svendsen Peninsula, central Ellesmere Island. In *Geology of the Canadian Arctic*. Aitken, J.D. and Glass, D.J. (eds).
- Miller, G.H., Bradley, R.S., and Andrews, J.T. (1975) The glaciation level and lowest equilibrium line altitude in the high Canadian Arctic: maps and climatic interpretation. *Arctic and Alpine Research* **7**: 155-168.
- Ó Cofaigh, C. (1997) Glaciation and sea level change, Raanes Peninsula, western Ellesmere Island, Arctic Canada. *Quaternary Newsletter* No. **82**: 40-41.
- Ó Cofaigh, C. (1998a) Geomorphic and sedimentary signatures of early Holocene deglaciation in High Arctic fiords, Ellesmere Island, Canada: implications for deglacial ice dynamics and thermal regime. *Canadian Journal of Earth Sciences* **35**: 437-452.
- Ó Cofaigh, C. (1998b) Configuration and dynamics of Late Wisconsinan glaciation in southern Eureka Sound, High Arctic Canada. *GSA Abstracts with Programs*, vol **30**, no. 7.

Ó Cofaigh, C. (1998c) Late Quaternary glaciation and postglacial emergence, southern Eureka Sound, High Arctic Canada. Unpublished Ph.D. thesis, University of Alberta, Edmonton, Alberta.

Powell, R.D. (1984) Glacimarine processes and inductive lithofacies modeling of ice shelf and tidewater glacier sediments based on Quaternary examples. *Marine Geology* **57**: 1-52.

Powell, R.D. (1990) Glacimarine processes at grounding-line fans and their growth to ice-contact deltas. In *Glacimarine Environments: Processes and Sediments*. Dowdeswell, J.A. and Scourse, J.D. (eds). Geological Society of London Special Publication No. 53, 53-73.

Powell, R.D. (1991) Grounding-line systems as second-order controls on fluctuations of tidewater termini of temperate glaciers. In *Glacial marine sedimentation; Paleoclimatic significance*. Anderson, J.B. and Ashley, G.M. (eds). GSA Special Paper 261, 75-93.

Reeh, N. (1984) Reconstruction of the glacial ice covers of Greenland and the Canadian Arctic Islands by three-dimensional, perfectly plastic ice-sheet modeling. *Annals of Glaciology* **5**: 115-121.

Sloan, V.F. (1990) The glacial history of central Cañon Fiord, west-central Ellesmere Island, Arctic Canada. Unpublished M.Sc. thesis, University of Alberta, Edmonton, Alberta.

Smith, I.R. (1998) Late Quaternary glacial histories and Holocene paleoenvironmental records from northeast and southwest Ellesmere Island, Nunavut, Canada. Unpublished Ph.D. thesis, University of Alberta, Edmonton, Alberta.

Stewart, T.G. (1988) Deglacial Marine Sediments from Clements Markham Inlet, Ellesmere Island, N.W.T., Canada. Unpublished Ph.D. thesis, University of Alberta, Edmonton, Alberta.

Stewart, T.G. (1991) Glacial marine sedimentation, Canadian High Arctic. In *Glacial marine sedimentation; Paleoclimatic significance*. Anderson, J.B. and Ashley, G.M. (eds). GSA Special Paper 261, 95-105.

Stuiver, M. and Reimer, P.J. (1993) Radiocarbon Calibration Program REV 3.0, *Radiocarbon* **35**: 215-230.

Thomas, G.S.P. and Connel, R.J. (1985) Iceberg drop, dump and grounding structures from Pleistocene glaciolacustrine sediments, Scotland. *Journal of Sedimentary Petrology* **55**: 234-249.

Trettin, H.P. (1987) Pearya: a composite terrain with Caledonian affinities in northern Ellesmere Island. *Canadian Journal of Earth Sciences* **24**: 224-245.

Tushingham, A.M. (1991) On the extent and thickness of the Innuitian Ice Sheet: a postglacial-adjustment approach. *Canadian Journal of Earth Sciences* **28**: 231-238.

Tushingham, A.M. and Peltier, W.R. (1991) Ice-3G: A new global model of late Pleistocene deglaciation based upon geophysical predictions of post-glacial relative sea level change. *Journal of Geophysical Research* **96**: 4497-4523.

Van der Veen, C.J. (1996) Tidewater calving. *Journal of Glaciology* **42** No. 141: 375-385.